RSC Advances

REVIEW

View Article Online
View Journal | View Issue

Cite this: *RSC Adv.*, 2022, **12**, 34766

MXenes and MXene-supported nanocomposites: a novel materials for aqueous environmental remediation

Md. Ahmaruzzaman *

Water contamination has become a significant issue on a global scale. Adsorption is a cost-effective way to treat water and wastewater compared to other techniques such as the Advanced Oxidation Processes (AOPs), photocatalytic degradation, membrane filtration *etc.* Numerous research experts are continuously developing inexpensive substances for the adsorptive removal of organic contaminants from wastewater. A fresh and intriguing area of inquiry has emerged as a result of the development of MXenes. This article aims to provide a preliminary understanding of MXenes from synthesis, structure, and characterization to the scope of further research. The applications of MXenes as a new generation adsorbent for remediation of various kinds of organic pollutants and heavy metals from wastewater are also summarized. MXenes with altered surfaces may make effective adsorbents for wastewater treatment. Lastly, the mechanism of adsorption of organic contaminants and heavy metals on MXenes is also discussed for a better understanding of the readers.

Received 2nd September 2022
Accepted 22nd November 2022

DOI: 10.1039/d2ra05530a

rsc.li/rsc-advances

1. Introduction

The first requirement for supporting life is water. Several industries emerged as a result of industrialization to make life easier.[1] The rate of water contamination is also rising rapidly as the rate of development does as well. Due to the daily increase in the amount of hazardous metals and organic compounds in wastewater, contamination of water is a threat on a global scale.[2,3] The textile, painting, mining, and metallurgy industries frequently discharge toxic chemicals, dyes-pigments, and heavy metals into the water systems.[4] In order to stop pollutants from getting into the food supply, it is essential to remove these dangerous substances from the water before discharging them into the surroundings.

As industrialization has progressed, environmental pollution has become more prevalent globally, posing substantial risks to ecology and human health.[4] The most common pollutants are toxic gases, organic chemicals, heavy metals, and bio-toxins. To deal with pollutants, several chemical, biological and physical techniques were developed, such as solvent extraction, membrane filtration, ion exchange, flocculation and adsorption.[3]

Heavy metal removal has become necessary due to their toxicity and harmful impacts on the ecosystem. Diverse methods, including as coagulation and flocculation, ion exchange, chemical precipitation, membrane filtration employing membranes (nanofiltration, reverse osmosis, ultrafiltration, and electrodialysis), oxidation, *etc.*, can be used to remove heavy metals. These techniques are pricey and have a number of drawbacks.[5] The chemical precipitation has limitations, such as development of secondary hazardous sludge, whereas, ion exchange has a narrow range of applications and has issues with resin fouling and regeneration. Large price of rehabilitation, low efficacy, production of hazardous wastes, requirements of considerable amount of coagulant, are some of the drawbacks of coagulation and flocculation process. Various filtration techniques utilizing membranes (reverse osmosis, electrodialysis, nanofiltration, *etc.*) have several limitations, such as limited lifetime of electrodes, necessity of membrane fouling, and high energy of membranes, demand of higher energy for electrodialysis.[5]

Among these techniques, adsorption is a promising method due to its ease of use, low cost, and economy.[6] Additionally, adsorption prevents secondary contamination caused by the production of dangerous compounds during regeneration process. Adsorbents with a greater surface area and functionality suited for adsorption process are typically used for efficient adsorption. Only a few porous materials have been developed as adsorbents for environmental pollutants, including chitosan, zeolites, Kaolinite, activated carbon, and metal–organic frameworks (MOF).[7,8] Hydrogel nanocomposites are also used as an excellent adsorbent for removal of aqueous pollutants.[9,10]

Several nanomaterials have recently demonstrated enormous potential in water decontamination because of their extraordinary physicochemical characteristics. MXenes, also known as 2-D transition metal carbides, nitrides, or carbonitrides, are a novel family of innovative nanomaterials that have

Department of Chemistry, National Institute of Technology, Silchar 788010, Assam, India. E-mail: mda2002@gmail.com

potential in both material science and water purification.[11] Recently, researchers were becoming interested in MXene, because of its distinctive architectures, outstanding stability, fine structure, and exceptional oxidation resistance high electrical conductivity, great chemical resistance, and being environmentally friendly.[11]

A MXene's structure can be defined as (n + 1) layers of transition metal elements M overlaying n layers of X (where X is a C or N element) as $(MX)_nM$ configuration. The existence of at least three distinct MXenes formulae—M_2X, M_3X_2, and M_4X_3 has been established.[12] Naguib *et al.*[12] explored the exfoliation of two-dimensional transition metal carbides in 2011 by selectively etching the "A" elements from the MAX phase. The suffix "ene" on these 2D-layered MXenes denotes their resemblance to graphene.[13] MAX phases, which are the precursors of MXenes, are systematically arranged nitrides and carbides of ternary metals are generally denoted as $M_{n+1}AX_n$, (MAX), where n varies in between 1 and 3, M is transition metal, A can be an element from groups 13 to 16 of the periodic table, such as Al, Ga, Ge, Si, *etc.*, and X may be either nitrogen, carbon, or a combination of the two. The almost densely packed M layers and the X atoms that occupy the octahedral positions in the layered hexagonal MAX phases are make up these phases.[14] A atoms hold the layers of M and X together. The M–X bond exhibits a combination of ionic, metallic, and covalent characteristics during the MAX phase, whereas the M–A bond typically has a metallic character.[15] MXenes comprise three or even more atomic layer thick two-dimensional materials that have different characteristics from respective 3-D parent precursor and are created by the controlled etching of A layers from MAX phases. MXenes are typically written as $M_{n+1}X_nT_x$, where n is typically between 1 and 3, and T denotes any functional groups (–O, –F, or –OH) that were produced as a consequence of the interaction with acids in the etching stage. The generated MXene has three potential lattice structures: M_2X, M_3X_2, and M_4X_3 (3, 5 or 7 atomic layers), depending on the MAX phases' n values, which range from 1 to 3.[16]

MXenes were suggested for usage in lithium-ion batteries, supercapacitors, semiconductor devices, and hydrogen storage.[17–20] MXenes work as efficient adsorbent materials for a variety of ionic or molecular species because of their hydrophilic properties and presence of relatively abundant surface functional groups. They can therefore be used for the treatment of environmental contamination. To the best of our knowledge, most of the review articles just summarize the synthesis and properties of MXenes for photocatalytic removal of pollutants, and no review article to date focused on the adsorption capabilities of MXenes as a new generation and efficient adsorbents for the removal of a wide range of organic contaminants and heavy metals from wastewater. We focus on the most current studies on MXenes for the adsorption of organic pollutants, such as dyes, medicines, organic chemicals, and heavy metals, and present a thorough description of those studies. We also describe the significant challenges coming up in the future to direct the recent research. A brief emphasis on the synthesis, structure and characterization techniques is also included in this article.

2. Structure, synthesis and characterization of MXenes and MXene-supported nanocomposites

2.1. Structure

MXenes share a hexagonal crystal structure with the fundamental MAX phase. $M_{n+1}AX_n$ is the typical formula for MAX

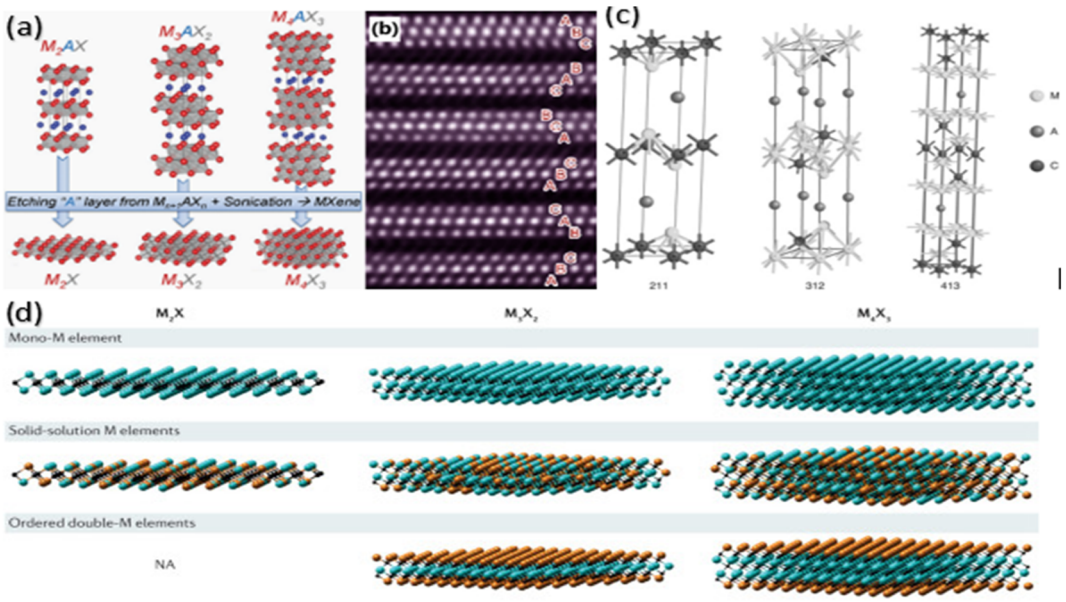

Fig. 1 (a) MAX phases 211, 312 and 413 crystal structures. (b) STEM-HAADF picture of a $Ti_3C_2T_x$ grain in the (120) zone-axis orientation. (c) Crystal structure of the M_3AX_2 phase with the $P6_3/mmc$ space group. (d) Mono-transition metal MXene, Solid solution-transition metal MXene, ordered-double MXene.[20,21,23,24]

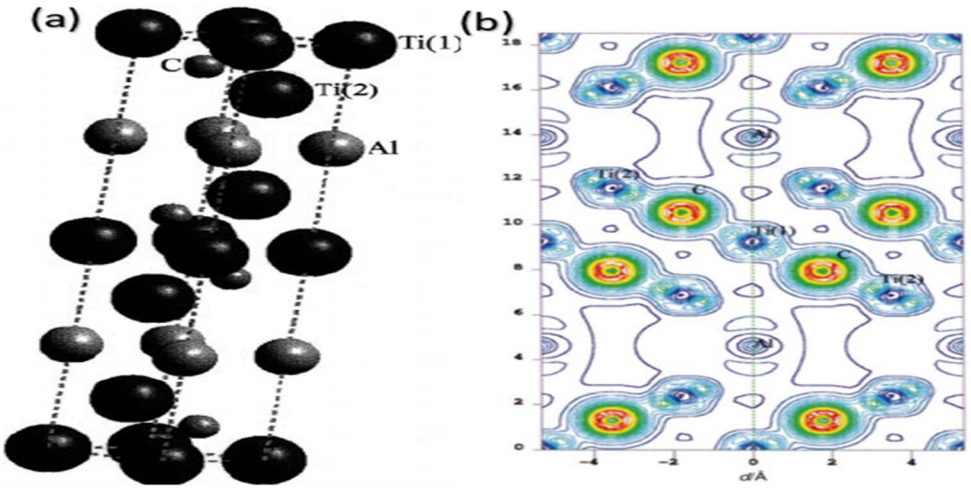

Fig. 2 (a) Crystal assembly and (b) charge density distribution pattern of Ti_3AlC_2.[25]

phases, which produces M_2AX (2 1 1), M_3AX_2 (3 1 2), and M_4AX_3 (4 1 3) (n = 1–3), as shown in Fig. 1a.[20] In all MAX phases, the "M" transition metal atoms organize into octahedra, and "X" atoms occupy these octahedral voids among the sheets of "M" atoms, creating M_6X interspersed with sheets of "A" elements, creating M_6X overlapping with sheets of "A" elements.[22] The only distinction between the "2 1 1, 3 1 2, and 4 1 3 phases" is the numbers of the "M atom layer between A atom layer." In summary, the layers of the MX and A alternatively occur during the MAX phase.

STEM-HAADF image of a MAX phase produced from the (120) plane in Fig. 1a and b layer acts as a mirror between two MX layers.[21] These MX layers are reproduced. MAX phases have a hexagonal crystal structure with two formula units per unit cell and $P6_3/mmc$ symmetry, as shown in Fig. 1c.[23] When the A layer is etched away out of the MAX phase, the remaining M layers with the X elements in their octahedral positions are known as 2D MXene sheets. These MXenes are mono transition metal MXenes, but after the discoveries of in-plane and out-of-plane ordered MAX phases in 2014 and 2017, respectively, "ordered double transition metal MXenes and ordered divacancy MXenes" have been found as depicted in Fig. 1d.[24]

Ti_3AlC_2 has a five-atomic sheet structure with a unit cell resembling a hexagon (Fig. 2a).[25] Three Ti sublayers containing carbon are arranged at the "octahedral interstitial sites" out of the five atomic sheets, and a reactive Al layer joins two neighbouring layers. The structure of $Ti_3C_2T_x$ is composed of the interlayer, intralayer skeleton, and the surface terminating groups zone. Fig. 2b depicts the Ti_3AlC_2 charge density distribution curve.[25]

2.2. Synthesis

The MAX phase is a collection of ternary nitrides or carbides which can be used to synthesize MXenes. These phases are composed of M, A, and X, which stand for an earlier transition metal, and A is an element from groups 13 or 14, and X is N or C, respectively.[26] Delamination and etching are frequently employed during the synthesis process. By the etching of A layers in MAX phase results in the typical MAX phase creation, $M_{n+1}AX_n$ (n = 1, 2, or 3), is changed into the multi-layered $M_{n+1}X_n$, probably as a result of A layers' inferior M–X bindings to M layers.[27] Following etching, delamination is done to create single-layered MXene by applying intercalants to enlarge the interlayer spacing and sonicating the final material to produce flakes or concentrations of a particular size and shape MXenes.[25]

By carefully etching the Al atomic layer with Ti_3AlC_2 as a precursor using aqueous HF at room temperature (RT), multilayer $Ti_3C_2T_x$ MXene can be created. Numerous studies have been conducted to develop new techniques for synthesizing MXenes.[28] By eliminating the Al layer from the Ti_3AlC_2 precursor, Naguib *et al.*[12] created a multilayer $Ti_3C_2T_x$ MXene using aqueous HF. The etching solution was then separated using vacuum filtering, and the material was obtained by washing with deionized water. By carefully regulating the HF concentration and etching time, they produced a sequence of MXenes structures. In order to create the $Ti_3C_2T_x$ multilayer Mxene structure, Halim *et al.*[29] used the Ti_3AlC_2 precursor in an aqueous solution of 1 M NH_4HF_2 and etched it for 120 h at RT. The resulted ultrathin single crystal Ti_3AlC_2 film was immersed in an aqueous solution of 1 M NH_4HF_2 and etched for 11 h RT to produce the $Ti_3C_2T_x$ MXene film. They have also discovered that in the course of an etching operation, tiny molecules or ions such as NH_3, NH_4^+, and others can naturally insert themselves through the MXenes layers, leading to the etching of A-site Al atoms.[29] A multilayer $Ti_3C_2T_x$ MXene was created by Wang *et al.*[30] utilizing NH_4F aqueous solution and a relatively safe hydrothermal technique. They also looked at the effects of etchant concentration, temperature, and reaction time on the yield of $Ti_3C_2T_x$ MXene.

Mashtalir *et al.*[31] have demonstrated that many cations, including Li^+, Na^+, Al^{3+}, Mg^{2+}, NH_4^+, and K^+, may be introduced spontaneously through multilayers of $Ti_3C_2T_x$ MXene. They demonstrated that etching reaction begins after 8 h of exposure to HF at 60 °C. Ghidiu *et al.*[32] used a risk-free and high-yield

approach to synthesize a multi-layered $Ti_3C_2T_x$ MXene. With the aid of magnetic stirring, they etched multilayer $Ti_3C_2T_x$ with clay-like characteristics for 24 hours at 35 °C. They utilized a solution of LiF and HCl as the etching agent. MXene materials are currently prepared using more advanced techniques, such as chemical liquid phase processes, chemical vapour deposition (CVD) processes, layering processes, and molten salt etching processes. These processes include HF substitution etching and HP etching processes.

2.3. Characterization

The visual examination is the initial stage of characterizing the MXenes, although its significance is sometimes undervalued in favour of the ultimate characterization of the MXenes product. Even in layered form, the transition from MAX to MXene results in a clear, noticeable colour change. Despite the fact that MAX phases are generally grey in colour, their structure and content, each MXene will have a unique hue that is related to its optical characteristics. When using delaminated MXenes, concentrated solutions have a black appearance; however, each MXene's unique colour is visible at dilute concentrations.

The colours of colloidal solution and thin-film have also been recorded for several MXene compositions,[33] and a change from the predicted hue is the first indication of MXene deterioration. For example, the "milky" or white appearance of solutions is an indication of oxidation and the generation of TiO_2 for Ti-supported MXenes. After MXene flakes have been removed, the colour of the supernatant can occasionally change because of soluble vanadium. This is further indication that MXene is degrading. If the MXene solution has begun to decompose, it should be thrown away since otherwise, the results won't be representative of the pure MXene. We must emphasize, nonetheless, that even in the event of MXene's anticipated visual appearance, accurate characterization of the substance using instrumental approaches must be carried out. This is covered in more detail below.

2.3.1 Fourier Transformed Infrared Spectroscopy (FT-IR). Since the interactions of the surface functional groups plays a role in the adsorption process, FTIR spectroscopy was used to examine the surface properties and hydrophilic makeup of the MAX phase and MXene, as illustrated in Fig. 2(b) and 3(a), respectively.[34] Fig. 3a shows the FTIR spectrum of the MAX phase, which illustrates the purity of Ti_3AlC_2 by the absence of any discernible peak. The FTIR spectrum of MXene, on the other hand, showed minute peaks at positions 1084 and 1728 cm^{-1}, 1408 and 2921 cm^{-1}, and a broad peak at positions 3000–3500 cm^{-1}. These positions correspond to the carbon to oxygen double bonds C=O and carbon to fluorine C–F bonds, while positions 1408 and 2921 cm^{-1} and broad peak at positions 3000–3500 cm^{-1}, respectively, to molecular water, C=O and OH bonds, respectively. While the intensity of the corresponding bonds is not robust and acute, describing their lower concentration,[35] the peaks belonging to the oxygen and fluorine-containing groups that were seen in the FTIR spectrum of MXene reflect their modest hydrophilic character.[36] Thus, fluorine and oxygen are found as surface terminal contaminants at very low concentrations on MXene. Three new peaks at 669 cm^{-1} (N–H stretching vibrations), 1041 cm^{-1} (Si–O–Si), and 1118 cm^{-1} (Si–O–Si) were observed in the FTIR spectrum of the MXene/PEI/SA (MPA) composite aerogel created by Feng *et al.*[37] demonstrating the success of the amino group and APTES fixation on the surface of MXene. When sodium alginate was utilised by Cui *et al.*[38] to functionalize the $Ti_3C_2T_x$ MXene surface, the FTIR spectra showed peaks at 1034 and 821 cm^{-1}, which were attributed to the C– and Na–O bonds, respectively.

2.3.2 X-ray Diffraction Analysis (XRD). X-ray diffraction is one of the oldest and easiest ways to verify MXene synthesis. The most effective method to precisely verify the purity of MAX phases is to use X-ray diffraction after significantly texturizing the powders.[39] The purity of its precursor material, MAX phase, should be ensured, precisely in the case of MXene. Because its coexistence in most commercial or scientific samples makes it

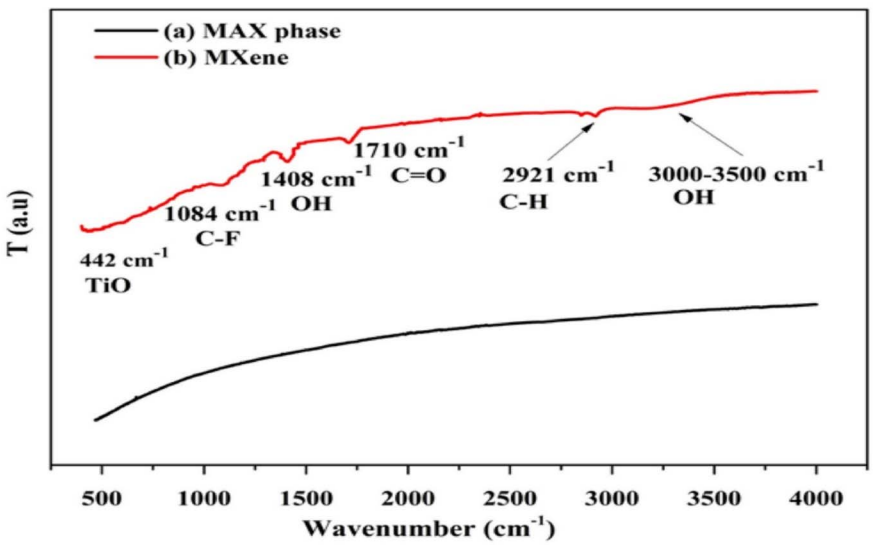

Fig. 3 FTIR spectra of (a) MAX phase (b) MXene.[34]

difficult to evaluate the findings. To confirm the advancements or modifications obtained in derived material, MXene is first required to characterize the source material. In XRD analysis, all peaks except the (0 0 2) peaks decrease or vanish as a MAX stage entirely transforms into MXene.[40] Additionally, in addition to a declining trend to lower angles and an increase in the d-spacing of layers, which showed a bigger *c* lattice parameter, there is also a broadening of the (0 0 2) peaks. The XRD results for the first MXene produced by Naguib and colleagues[12] ($Ti_3C_2T_x$) showed that the major peak's position had changed from 40° to 10°.[41] The MAX and MXene patterns are present in almost every article on MXene, typically with no additional study or thought other than to demonstrate that the MAX was topochemically transformed to MXene.[39] The impact of etching factors on the final design and characteristics of MXenes has been examined, among other XRD-related studies.[42] The characteristics of MXenes can be modified using XRD to overcome existing constraints and further our understanding of these compounds.

2.3.3 Raman spectroscopy. The structures of 2-dimensional materials have been extensively studied using vibrational spectroscopy methods because they are powerful tools for identifying molecular imprints. As a result, when elucidating a vibrational spectrum, symmetries of the materials must be taken into consideration. The geometry of MXene is deformed $P6_3/mmc$ and brought on by surface groups, widens vibrational bands. The material's photon dispersion determines the band position. This is normally determined by DFT modelling and was researched for several MXenes.[43,44]

Because simulation only includes one-unit cell, the attainable forecasts rely on the structure, where it accepts uniform surface groups. The MXene production process really results in a variety of surface groups that are distributed randomly throughout the flake. This enables the superposition of vibrations of the surface groups, peak widening, overlapping, and rendering interpretations of Raman spectra very complicated.

The presence of MXene in the composites was verified using Raman spectroscopy. Raman spectroscopy was used to confirm that MXene was present in the composite materials.[45] It is possible to trace spectral signatures thanks to the technique's distinctive fingerprint and resolving power. The approach sensitivity allows for assessment of structure and functional groups on the surface of MXene, even though various synthesis techniques are applied. The impacts of MXene degradation have been studied, and it has been utilized to monitor material oxidation.[46]

2.3.4 Scanning electron microscopy. Scanning electron microscopic technique enables examination of the architecture even if not all etched samples have the same appearance and frequently provides clear evidence that MXene is created. The "accordion" shape is thought to be a sign of a successful synthesis since the initial MXenes were created by submerging in extremely concentrated hydrofluoric acid. This "accordion" shape, which is now largely synonymous with MXene, does not, however, fully capture the appearance of multilayer MXene. Fig. 4 illustrates the SEM images of $Ti_3C_2T_x$.[47]

2.3.5 Atomic force microscopy (AFM). Atomic force microscopy (AFM) has gained a lot of interest in the

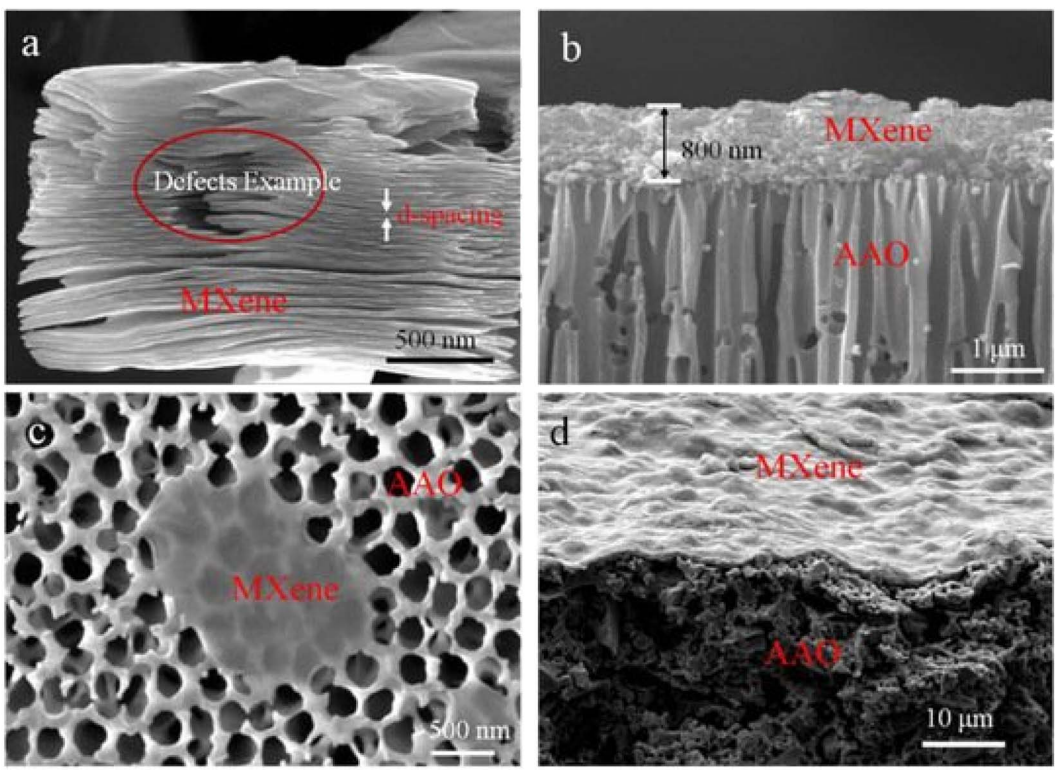

Fig. 4 (a and b) SEM images of cross-section of $Ti_3C_2T_x$ (c) Top view and (d) low magnification cross section.[47]

investigation of 2D materials it can indicate the lateral flake size and thickness. However, one should be mindful of the restrictions while doing AFM investigations because the thickness of 2-dimensional monolayers can vary significantly based on the presence of various surface adsorbed species and entrapped interfacial molecule, besides the imaging method involved.[48] Moreover, rather than using a flake on the substrate, it is frequently possible to measure the height of the two layers, such as folded portions of the sample, in order to determine the depth of a single 2-dimensional layer of the materials with greater accuracy.[49]

MXenes are comparable to that of other 2D materials in this respect. For instance, it was established that the second layer of $Ti_3C_2T_x$ was 1.6 nm high as opposed to approximately 3.0 nm high for the MXene layer, which was applied directly to the Si/SiO_2 substrate.[50] This is nevertheless an overestimation compared to the nominal thickness of approximately 1 nm, which was determined by high-resolution TEM and anticipated by computational modelling.[51,52] For this reason, the preferred method for measuring monolayer thickness is cross-sectional TEM. There haven't been any studies of MXenes using scanning tunnelling microscopy so far.

2.3.6 X-ray photoelectron spectroscopy. The most advanced spectroscopic technique for figuring out the typical material composition is XPS. XPS has become more and more popular for surface analysis due to its minimum depth of penetration, surface sensibility, and ability to reveal the chemical composition of the surface and elemental oxidation state. This has been used to research the composition and surface chemistry of various MXenes, the intercalation process, and the thermal stability of the surface groups of the materials.[53,54]

The XPS spectra for the Ti 2p, O 1s, and F 1s regions for $Ti_3C_2T_x$, MX–Na, and MX–Na–A are shown in Fig. 5a–c along with their peak-fits.[55] The peak placements, FWHMs, peak area percentages, and peak assignments determined by fitting technique. The peaks designated TiO_2 and $TiO_{2-x}F_x$ are also attributed to Ti atoms found in surface oxides, oxyfluorides, and/or Ti adatoms attached to O atoms on the surface of MXene.

The related components C–Ti–O(I)$_x$, C–Ti–O(II)$_x$, C–Ti–(OH)$_x$, Al(OF)$_x$, and H_2O_{ads} were used to fit the O 1s region of $Ti_3C_2T_x$ (Fig. 2b, bottom curve). The C–Ti–O(I)$_x$ and C–Ti–O(II)$_x$ peaks were identified as the fcc site (also known as the A site) and MXene bound O bridging two Ti sites, respectively. Peaks with the labels C–Ti–(OH)$_x$ and H_2O_{ads} were attributed to OH terminations linked to MXene and water, respectively. The remaining O 1s area is associated with the peak "Al(OF)$_x$," which was attributed to O in aluminium oxyfluoride, an etching by-products.

The same elements, in addition to $TiO_{2-x}F_x$, which are surface oxyfluorides, were used to match the O 1s area of MX–Na (Fig. 2b, middle curve). As indicated in Fig. 5b, after annealing, the proportion of MXene bound O (C–Ti–O(II)$_x$, C–Ti–(OH)$_x$, and $H_2O_{ads.}$) increased from 47% of the O 1s region before annealing to 56% of the O 1s region. Two peaks of BEs at 685.4 and 687.5 eV were used to fit the F 1s region of $Ti_3C_2T_x$ (Fig. 2c lower

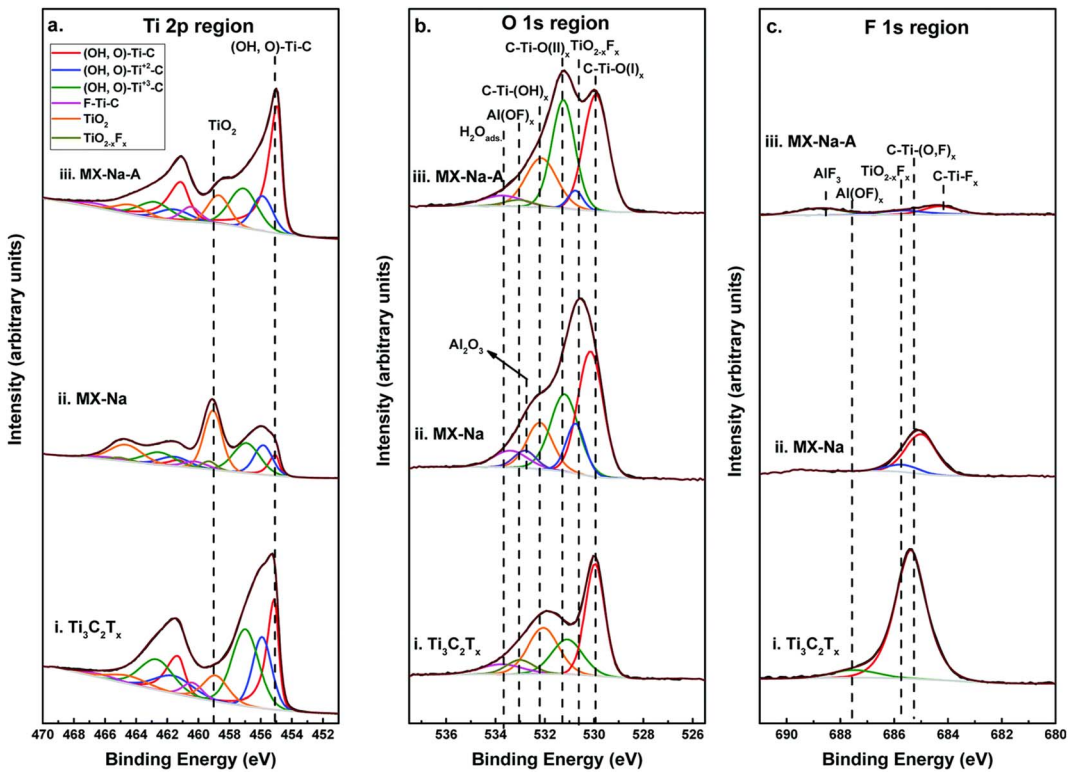

Fig. 5 XPS spectra with curve-fitting for (a) Ti 2p region for (i) $Ti_3C_2T_x$, (ii) MX–Na (iii) MX–Na–A. (b) O 1s region for (i) $Ti_3C_2T_x$, (ii) MX–Na (iii) MX–Na–A. (c) F 1s region for (i) $Ti_3C_2T_x$, (ii) MX–Na (iii) MX–Na–A.[55]

curve). $Ti_3C_2T_x$ contains F linked to Ti, C, and O atoms, and this peak makes up the majority of the "C–Ti–$(O,F)_x$" peak, which comprises 97% of the F 1s area. The F species in Al oxyfluorides, a consequence of the etching process, are represented by the second, almost insignificant peak labelled $Al(OF)_x$.

3. Adsorption of contaminants on MXene and MXene-based nanocomposites

3.1. Pharmaceuticals

Pharmaceutical compounds, which are widely used in the treatment and prevention of diseases in humans and animals, are in greater demand as living standards rise.[56] Due to their permanence, toxicity, and mobility, pharmaceutical chemicals found in water can harm plants, animals, and humans.[57,58] In 2019, groundwater utilized for drinking in the United States contained 103 different types of pharmaceutical chemicals, according to the United States Geological Survey.[59] More research have shown that traditional water and wastewater treatment facilities cannot effectively remove pharmaceutical drugs, which results in the discharge of diverse pharmaceutical compounds, including effluents, into different water resources.[60] In other words, a number of current water issues are brought up by the presence of pharmaceutical compounds in water. Therefore, the removal of pharmaceuticals is of utmost concern.

Recently, Kim *et al.*[61] investigated the application of $Ti_3C_2T_x$ MXene for the adsorptive removal of amitriptyline (AMT), verapamil (VRP), carbamazepine (CBM), 17 α-ethinyl estradiol (EE2), ibuprofen (IBP), and diclofenac (DCF) from aqueous phase in presence of various inorganic and organic compounds. The maximum adsorption capabilities of 138 mg g^{-1} for AMT could be achieved for un-sonicated $Ti_3C_2T_x$ at neutral pH. As expected, the adsorption efficiency decreases in the presence of other contaminants due to competition between ions and target drug molecules for adsorption over the adsorbent surface. However, the adsorption capability with surrounding background inorganic ions was lesser than that without ions since the background inorganic ions blocked the electrostatic attraction between AMT and $Ti_3C_2T_x$.

In another study, Ti_2C MXene exhibits outstanding adsorption efficiencies of 44, 100 and 88%, towards ampicillin, cloxacillin, and amoxicillin, adsorption from aqueous solutions.[62] The authors concluded that the MXenes with a higher concentration of surface functional groups could be more efficient for the adsorption of pharmaceuticals from wastewater. The Gibbs free energy and adsorption energy profile after interaction of cloxacillin with functionalized Ti_2C were shown in Fig. 6.[62]

A novel sodium-ion intercalated $Ti_3C_2T_x$ MXene was employed for the adsorption of 10 ppm ciprofloxacin (CFX).[63] About complete adsorption of CFX was observed within 20 min of treatment. The enhanced adsorption efficiency of sodium incorporated MXene compared to pristine MXene was attributed to the increased spacing between the layers and a greater number of active sites. The stability of the prepared MXene was investigated *via* XRD and SEM analysis which did not reveal any significant structural changes after eight cycles of adsorption and electrochemical regeneration.[63] In a similar finding, sodium intercalated Ti_3C_2 MXene-TiO_2 (MX-TiO_2) showed enhanced adsorption of enrofloxacin (ENR) from an aqueous stream.[64] The addition of NaCl during hydrothermal synthesis of Ti_3C_2 from $Ti_3C_2T_x$ slowed down the formation of TiO_2 and resulted in the formation of sodium intercalated MXene, which increased the adsorption capacity from 1 to 6 mg ENR per g composite. This was brought on by sodium intercalation into the MX structure, which enables ENR uptake *via* cation exchange mechanism. Additionally, the presence of NaCl affects the quantity of TiO_2 that forms, slowing it down (small anatase crystallite size and aggregate TiO_2 amount), while distributing it more uniformly throughout the composite structure, in comparison to the systems without NaCl at similar temperature.

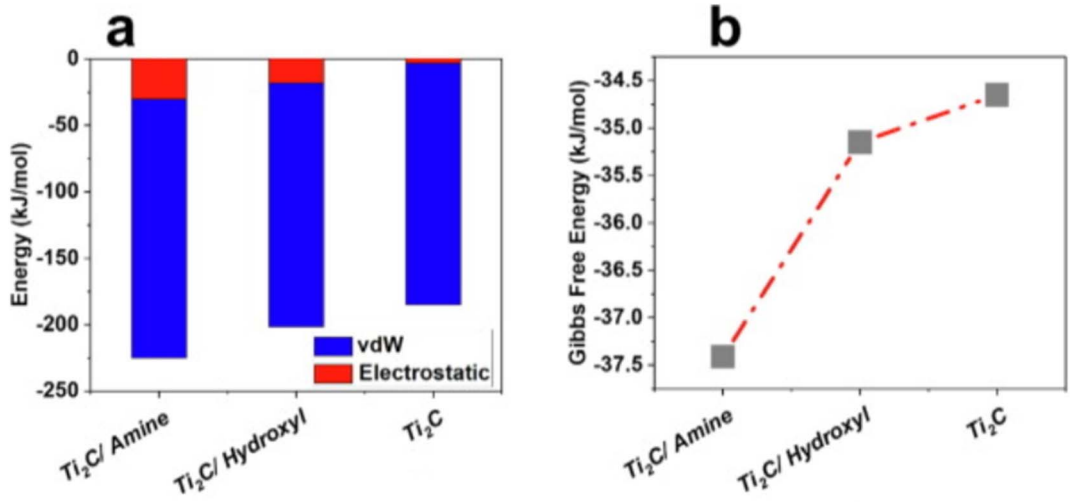

Fig. 6 (a) Gibbs free energy and (b) adsorption energy profiles after the interaction of cloxacillin with functionalized Ti_2C (vdW = van der Waals interaction).[62]

Xu *et al.*[65] used magnetic Fe_3O_4@MXene nanocomposite for the adsorption of 17α-ethinylestradiol (EE2) from water. Under the optimum condition of pH = 6.5, pollutant dosage of 0.98 mg L^{-1}, and the adsorbent dosage of 89.9 mg L^{-1}, about 96% of EE2 could be effectively removed from the solution. The quadratic model was used to optimise the process variables for the highest adsorption of 17α-ethinylestradiol by Fe_3O_4@Ti_3C_2. The maximum adsorption of 97.08% that the model predicted under the ideal conditions for the independent variables (adsorption period of 6.7 h, pH of the solution at 6.4, initial EE2 concentration of 0.98 mg L^{-1}, and adsorbent dose of 88.9 mg L^{-1}) was extremely similar to the experimental value (95.34%). In comparison to other components, pH demonstrated the highest level of importance with a percent contribution (63.86%). Significant (p 0.05) interactions between pH and starting concentration affected EE2 adsorption efficiency. The process parameters for the adsorption of EE2 were optimally chosen using the response surface methodology, which successfully captures the effects of many factors. Up to equilibrium, the EE2 removal efficiencies (%) rose as the time passed. In the pH range of 4 to 10, the impact of initial solution pH on EE2 adsorption was examined. Given that the adsorbent contains hydroxyl groups and that Fe_3O_4@Ti_3C_2 has a skeleton, it is possible to assume that hydrogen bonds and hydrophobic forces will predominate during adsorption.[66] As a result, moderate pH conditions are preferred for EE2 adsorption.[67] The adsorption of EE2 on Fe_3O_4@Ti_3C_2 was dominated by the pseudo-second-order kinetic. The Langmuir model provided an accurate description of the experimental adsorption data. The adsorption process was endothermic and spontaneous, according to a thermodynamic analysis. The produced Fe_3O_4@Ti_3C_2 shown high EE2 water solution absorption efficiency, indicating its potential for use in real-world environmental remediation applications. Since MXene contains aromatic rings, it has higher hydrophilicity, hence hydrophobic partitioning cannot be taken into account in this study. EE2 contains aromatic ring and phenolic hydroxyl groups, and that MXene Ti_3C_2 has terminals made up of –OH, –O, and/or the –F surface, it is reasonable to assume that hydrogen bonding will be the primary mechanism guiding adsorption. Fe_3O_4@Ti_3C_2 also exhibits good magnetic characteristics, making it a promising new adsorbent for removal of EE2 from water and wastewater.

Alkaline intercalation was used to create surface hydroxylated MXene and used for the adsorption of Tetracycline (TC).[68] The alkalization procedure improved the interlayer gap of MXene whilst maintaining the layered structure, according to SEM and XRD. Surface F was converted to surface OH, as demonstrated by EDS and XPS. Batch adsorption measurements show that adding metal ions significantly boosts the adsorption efficiency of TC by altering the surfaces of alk-MXene by free heavy metal ions from the surrounding aqueous environment. Additionally, the results of the model-fitting calculations showed that the adsorption procedure adheres to the Freundlich adsorption model. UV-vis and XPS analyses showed that the surface hydroxyl group of alk-MXene was the adsorption site, and modification of the surface metal ions and further improvements by complexation are the prime causes for significantly increased the adsorption of Tetracycline. A plausible adsorption mechanism was finally put forth, and it could be a competitive strategy to utilize an extraordinary active surface and certain constituents present in wastewater to remove diverse contaminants in a synergistic way.

3.2. Dyes

Due to their toxicity, organic dyes are among the most predominant contaminants in wastewater. Dye molecules often have stable molecular structures, making them resistant to biological degradation. Wastewater comprising dyes is a significant environmental contaminant that also negatively impacts human health because of the large-scale production of highly coloured wastewater of the textile industry containing a variety of persistent contaminants.[69]

The charged state of the dye is important for the adsorption of dyes on MXenes. The use of MXenes to remove dyes from water has been reported to be highly effective.[70,71] Many researchers have investigated the idea of employing MXenes for removing dyes from water. MXenes offer a variety of sites for the adsorption of dyes because of their significantly higher surface area and presence of active functional groups on the surface.[70,71]

Jun *et al.*[72] used $Ti_3C_2T_x$ MXene to remove methylene blue (MB) and acid blue 80 (AB) dyes from simulated wastewater. The isoelectric points and surface areas of $Ti_3C_2T_x$ MXene were roughly pH 3 and 9 m^2 g^{-1}, respectively. Thus, when the concentrations of the adsorbents and adsorbates were 25 and 10 mg L^{-1}, respectively, MXene shown significant capacity for MB (140 mg g^{-1}) adsorption because of their electrostatic interactions. Although, MB could strongly and irreversibly bind to $Ti_3C_2T_x$, AB80 could only showed seldom adsorption towards AB. The cationic dye adsorbs over the anionic dye preferentially in aqueous solutions because of the electrostatic attraction between the positively charged cations of the dye and the negatively charged surfaces of MXenes. $Ti_3C_2T_x$ showed an enhanced adsorption capacity of MB higher than that of Kaolinite.[73] Fast kinetics and great selectivity were displayed by MXene in the elimination of MB. The presence of divalent cation, anion, and humic acids, pH of the solution, ionic strength, along with FT-IR and XPS spectroscopic analyses provided a clear explanation for the adsorptive removal of MB on $Ti_3C_2T_x$.

Treatment of $Ti_3C_2T_x$ by LiOH and NaOH increased interlayer spacing by 29% and 28%, respectively, according to Wei *et al.*[74] Comparing pure $Ti_3C_2T_x$ MXene without the alkali treatment, the adsorption capabilities of NaOH–$Ti_3C_2T_x$ and LiOH–$Ti_3C_2T_x$ for methylene blue are 189 and 121 mg g^{-1}, respectively (100 mg g^{-1}). While LiOH–$Ti_3C_2T_x$ had a larger interlayer spacing and a thinner sheet, NaOH–$Ti_3C_2T_x$'s SEM imaging was similar to that of pristine $Ti_3C_2T_x$ (sheet thickness of 40 nm).[74] The MB removal rates of NaOH–$Ti_3C_2T_x$ (100%), LiOH–$Ti_3C_2T_x$ (100%) and KOH–$Ti_3C_2T_x$ (70%) were significantly greater than $Ti_3C_2T_x$ due to the abundance of OH groups (50%). $Ti_3C_2T_x$ (100 mg g^{-1}), KOH–$Ti_3C_2T_x$ (75 mg g^{-1}), and LiOH–$Ti_3C_2T_x$ had lower adsorption capacities (121 mg g^{-1}) than that of NaOH–$Ti_3C_2T_x$ (189 mg g^{-1}).

Two different types of 2D MXenes, such as Ti_3C_2 and Nb_2C were produced through a hydrothermal etching process between $NaBF_4$ and HCl in the absence of using HF directly.[75] The HF served as a source of fluoride to etch the MAX phase processor, and make corresponding MXene, which consists of Ti_3C_2 and Nb_2C. The hydrothermal approach, as opposed to the conventional HF etching procedure, provided a higher degree of Al layer ablation and a longer interlayer spacing of 2D MXenes, allowing for simple sonic exfoliation. The MXenes produced using the hydrothermal etching procedure had a greater BET surface area than those produced using the conventional HF etching method and showed improved adsorption performance for methyl orange and methylene blue. The ubiquitous, secure, and effective method for the synthesis of 2D MXene materials presented in this work may open up new opportunities for the general use of 2D MXenes.[75]

After immersing $Ti_3C_2T_x$–COOH into PEI and then PAA solution, MXene ($Ti_3C_2T_x$–COOH@[PEI/PAA]) nanocomposites with carboxylated core–shell structures were developed using the layer-by-layer (LBL) method.[76] The resultant MXene-COOH@$(PEI/PAA)_n$ composites could effectively adsorb Methylene blue (MB), Safranine T (ST), and Neutral red (NR) because of the distinctive composite layer topologies and different chemical groups in the hierarchical core–cell architectures of the developed composites. The cycle adsorption studies were performed eight times in a row using the identical composite material and brand-new MB dye solution. The investigations show that, in contrast to 85.6% m in the initial adsorption phase for MXene-COOH@$(PEI/PAA)_{10}$ composite, the removal rate towards MB sustains at roughly 64.4% after eight consecutive cycles. The composites produced in this study exhibit excellent stability and reusability. Additionally, due to a little loss of surface by-product deposition or repeated washing on the composite surface, the adsorbent's adsorption effectiveness somewhat declined after a number of cycles.[76]

It was possible to create T-$Ti_3C_2T_x$ sheets with terephthalate supports by mechanochemically eliminating the MAX phase.[77] A large surface area (135.7 m^2 g^{-1}) and outstanding MB adsorption capacity are displayed by the developed T-$Ti_3C_2T_x$ due to the increased interplanar space and accessible availability of terephthalate. Then, utilizing aromatic-coupling-diazotization, MXene with sulfonic groups functionalization (Ti_3C_2–SO_3H) was created in order to test their MB adsorption potential.[78] Ti_3C_2–SO_3H nanosheets were produced, as seen in SEM pictures (Fig. 7). The larger percentage of MB removed explains why the adsorption process was facilitated by higher initial dye concentration and temperature. The composite's greatest recorded adsorption capacity, 111 mg g^{-1}, was obtained in 70 min, less quickly than Ti_3C_2 (21.10 mg g^{-1}). A 2D Ti_3C_2 functionalized magnetic Fe_3O_4 (2D-MX@Fe_3O_4) composite was made using the *in situ* growth method and utilized for adsorption of MB from water.[79]

The elemental distribution of 2D-MX@Fe_3O_4 showed that Fe was present alongside Ti, O, and C. The lamellar structure decorated with Fe_3O_4 nanoparticles was found to contain iron, oxygen, titanium and carbon, according to the results of the elemental mapping study (55 nm).

The produced complex 2D-MX@Fe_3O_4 displayed a typical 2D lamellar structure with a superparamagnetic characteristic of 20.3 emu g^{-1}. A negative charged surface of 2D-MX@Fe_3O_4 at neutral medium was revealed by zeta potential measurement, which was advantageous for cationic dye removal.[79] Furthermore, compared to lower temperatures, the removal procedure demonstrated a superior decolorization at a high temperature of 91.93% (55 °C). At high temperatures (40 and 55 °C), the removal of MB was shown by adsorption isotherm to fit the Freundlich isotherm model well, however at low temperatures (25 °C), the removal was shown by Langmuir isotherm. The removal of MB was shown to be an exothermic and chemisorption process by thermodynamic analysis, which also showed that a rise in temperature could significantly boost the removal efficiency of 2D-MX@Fe_3O_4. The adsorption mechanism at high and low temperatures was further investigated using FT-IR, XRD, and XPS techniques.[79] While surface adsorption *via* electrostatic interaction contributed to the MB removal process in the case of 25 °C, the abundant Ti–OH

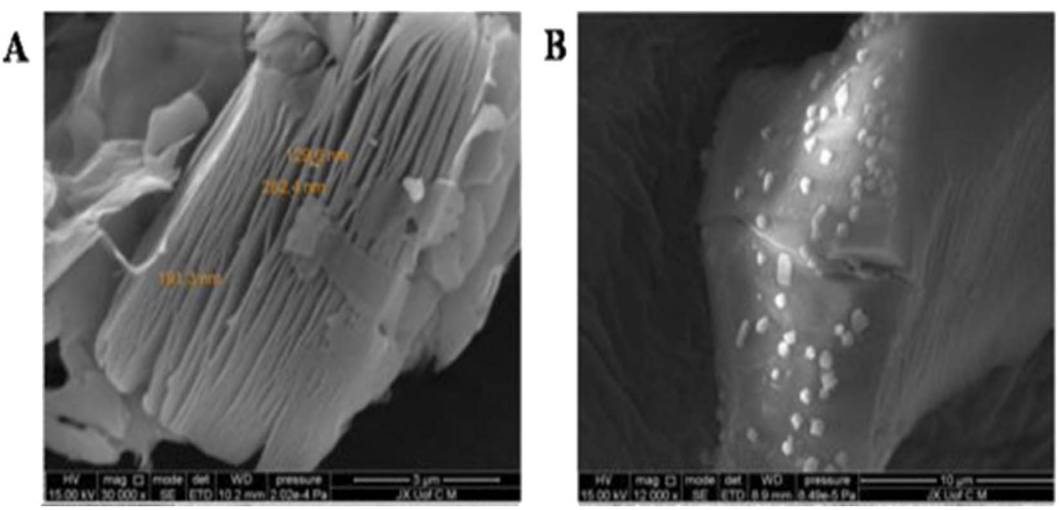

Fig. 7 SEM images of (A) pristine Ti_3C_2 and (B) Ti_3C_2–SO_3H.[78]

groups on the surface of 2D-MX@Fe_3O_4 played a major role in improving the MB decolorization through hydrogen bonding (Ti–OHN) and electrostatic attraction at high temperature systems. The Ti_3C_2@Fe_3O_4 composite showed good stability and reusability after five cycles.[79]

Rhodamine B (RhB) and MB were more effectively adsorbed by the "phytic acid (PA)-doped ($Ti_3C_2(OH_xF_{1-x})_2$) (PA-MXene) composite" synthesized by "rod-like $Ti(OH)PO_4$ and ($Ti_3C_2(OH_xF_{1-x})_2$)" utilizing a hydrothermal procedure for 12 h.[80] SEM scans reveal a rod-like structure for PA-Ti_3C_2-12. PA-Ti_3C_2-12 composite showed greater adsorption capabilities toward rhodamine B (22.1 mg g^{-1}) and methylene blue (42.3 mg g^{-1}) in comparison to that of pure MXene and was explained by the increased surface area and enough oxygen availability. The adsorption process was endothermic as the temperature increased, indicated by increased adsorption capacity. The adsorption isotherms of PA-Ti_3C_2-12 followed the Langmuir isotherm pattern with a K_L of 1.1288 L mg^{-1}.

$Ti_3C_2T_x$ MXene was synthesized by Kadhom *et al.*[81] and studied the removal of Malachite green. The adsorption procedure was regulated using the Freundlich isotherm and pseudo-second-order kinetics. The percentage removal efficiency increased when the adsorbent dose was raised, achieving 94% at a dosage of 1.8 g L^{-1}. This is explained by the leuco nature of dyes. The removal efficiency initially increased significantly with time, reaching equilibrium within 60 min and decreased with increase in initial concentration of the dye. Magnetic nanospheres made of MXene@Fe_3O_4@CS were synthesised using ultrasonic self-assembly for the removal of Congo Red (CR) from water.[82] It was shown that CR has an adsorption capacity of 620.22 mg g^{-1}. According to the authors, the adsorption process was endothermic, entropy-driven, and spontaneously thermodynamic.

Tetramethylammonium hydroxide (TMAOH) was employed in a different investigation to intercalate and delaminate multilayered $Ti_3C_2T_x$ in order to produce $Ti_3C_2T_x$ MXene nanosheets solution.[83] The nanocomposites displayed excellent performance for the removal of methylene blue with the highest adsorption capacity being 1026 mg g^{-1} at 318 K. The produced $Ti_3C_2T_x$ MXene composites could be promising absorbents for absorbing methylene blue.[83]

Polypyrrole (PPy) has also been shown to be an effective adsorbent for the removal of organic dyes due to the presence of π-conjugate structures and nitrogen atoms with positive charges in the PPy substrate.[84] This endows PPy with multiple interactions with pollutants in wastewater through hydrogen bonding, electrostatic interactions, and π–π interactions.[85] Therefore, it can be concluded that the adsorption ability of PPy nanoparticles may somewhat compensate for the potential lower adsorption capacity related to the reduction of active site on MXene nanosheets caused by the occupation of PPy nanoparticles. In this regard, Shi *et al.*[86] synthesized few-layered MXenes/PPy composite particles and used for the removal of MB from aqueous phase. It was indicated that adding PPy nanoparticles encourages MXene to exfoliate even more. As a result, the adsorption capacity of the MXene/PPy composites is significantly increased and reaches a maximum of 553.57 mg g^{-1}. Additionally, the MXene/PPy composites exhibit remarkable selectivity towards adsorption and extract only methylene blue from aqueous solution while simultaneously combining with cationic and anionic dyes. The MXene/PPy composite particles exhibit almost no oxidation and significantly improved MXene stability. The MXene/PPy nanocomposites also showed remarkable selectivity, combining anionic and cationic dyes while only eliminating MB from the aqueous phase. The MXene/PPy composites demonstrated nearly no oxidation, and the MXene's stability has been greatly increased. This study presents a novel technique for producing very stable composite adsorbents based on MXene that have the potential for effluent water treatment.[86]

A new AA-alkaline-MXene adsorbent was produced by grafting acrylic acid (AA) on alkalized single-layered MXene nanosheets and showed excellent adsorption performance for methylene blue and congo red.[87] XPS, XRD, TGA, and Raman spectroscopic investigations confirmed that grafting of AA on the alkalized MXene nanosheets was successful. The highest adsorption capacity of PAA2-alk-MXene for CR and MB was 264.46 and 193.92 mg g^{-1}, respectively, at $T = 328$ K and $C_0 = 90$ mg L^{-1}. The adsorption of MB and CR on the surface of homogeneous PAA2-alk-MXene falls within the category of monolayer adsorption, and the process was guided by the "Langmuir isotherm and pseudo-second-order model.[87] Because CR contains more functional groups that are active, such as nitrogen/oxygen functional groups, sulfonate groups, and other functional groups, the sample's overall adsorption performance for CR is higher than it is for MB. Adsorption mechanism revealed that the main forces acting on the AA-alk-MXene and the dyes were electrostatic force of attraction, hydrogen bonding, and intercalation adsorption.

Yan *et al.*[88] successfully developed Nb_2CT_x MXene through etching Nb_2AlC with HF, with a high specific surface area of around 44.69 m^2 g^{-1}. Both cationic (MB) and anionic dyes (MO) can be effectively absorbed by the as-prepared Nb_2CT_x MXene. The highest adsorption capacities of MB and MO dyes were 496 and 493 mg g^{-1} from an initial concentration of 500 mg. L^{-1}, pH = 7 and adsorbent dose of 1 g L^{-1} of Nb_2CT_x MXene. The chemisorption at active "adsorption sites" is the rate-limiting phase in the adsorption process of Nb_2CT_x MXene, which also follows a pseudo-second-order kinetics model. Their findings offer insight into the future engineering of better MXene-based absorbents and demonstrate that Nb_2CT_x MXene is a good candidate for a highly efficient adsorbent for removal of dyes from wastewater.[88]

Wu and his research group created CPCM@MXenes,[89] a superabsorbent material inspired by pods, in 2022. The composites were made using $Ti_3C_2T_x$ MXene formulas derived from the Ti_3AlC_2 MAX phase and chitosan-functionalized porous carbon microspheres (CPCM). In order to prevent them from agglomeration and to produce a large surface area (>1800 m^2 g^{-1}). To eliminate crystal violet from water, CPCM@MXene, with extremely effective adsorbent capacity, was investigated.[89] The maximum adsorption capacity reached 2750 mg g^{-1}. Hydrogen bonds, physical adsorption, stacking effect, and electrostatic interactions all contribute to

understanding the adsorption mechanism. The remarkable adsorption efficiency of CPCM@MXenes for eliminating crystal violet may be applied to other molecular pollutants using a model aquatic environment. These super absorbents are also highly recyclable, making it simple to reuse them.

RhB and MB dyes can both be removed from aqueous solutions using a different two-dimensional material called "stack-structured magnetic Fe_3O_4 nanoparticle attached titanium carbide MXenes ($Ti_3C_2T_x/Fe_3O_4$)".[90] The synthesized $Ti_3C_2T_x/Fe_3O_4$ composites demonstrated highest adsorption capacity of 86 and 153 mg g^{-1} for the Rh B and MB, respectively. The single layer adsorption of RhB and MB on the adsorption sites of $Ti_3C_2T_x/Fe_3O_4$ is indicated by the Langmuir model, which closely matches the results of batch adsorption experiments. The produced composites also displayed quick RhB/MB adsorption kinetics.[90] The presence of magnetic Fe_3O_4 nanoparticles was attributed to the generated composites' outstanding stability and ability to be recycled up to four times. In the authors' opinion, the remarkable adsorption abilities of $Ti_3C_2T_x/Fe_3O_4$ make it a viable candidate for effectively removing cationic dyes from water.[91] 10 mg of the produced $Ti_3C_2T_x/Fe_3O_4$ composites had the ability to eliminate more than 96.8% of MB in 30 minutes, 83.4% of rhodamine B, and 44% of methyl orange in 120 min from an initial concentration of 50, 25, and 20 mgL^{-1}, respectively. It has stronger adsorption and degradation capacities for a range of dyes when used in small doses. HF-forming etchants were used to produce Ti_3C_2 MXenes, which were then alkalized to swap out the –F for terminal functional groups that included oxygen.[92] When ML-Ti_3C_2 was alkalized, it transformed into ML-$Ti_3C_2(OH)_2$, a substance with a considerable increase in functional groups containing oxygen and porosity over ML-Ti_3C_2. Then, ML-$Ti_3C_2(OH)_2$ was used to adsorb MB and achieved adsorption–desorption equilibrium with MB within 30 minutes in complete darkness, and over the course of 120 min, when exposed to visible light, 81.2% of MB was selectively degraded from an initial concentration of 10 mg L^{-1}. Based on the radical quenching studies, a potential degradation mechanism was formulated.[92]

3.3. Miscellaneous organic contaminants

Pesticides have become a necessary component of modern civilization and are applied to protect agricultural land, food storage facilities, flower gardens, in addition to get rid of pests that spread infectious diseases that are dangerous to humans.[93] Numerous elements of the water, air, and soil ecosystem have been contaminated by the continual application of persistent and non-biodegradable pesticides. Additionally, pesticides have bioaccumulated in the upper tropic level of the food chain. More recently, exposure to pesticides has been linked to a number of acute and chronic human disorders.[94] Pesticides are specific chemical substances used to prevent, eradicate, or control pests, illnesses, and weeds that plague forestry and agriculture. Regarding chemical composition, pesticides can be broadly classified as organic and inorganic. Among other elements, copper, sulphur, and other substances make up inorganic insecticides. In our daily lives, we are most familiar with organochlorine pesticides (OCPs) and organophosphorus pesticides (OPPs). Recently, for the first time, flower-like MoS_2@MXene has been investigated for the adsorption of pesticide paraquat dichloride (PQ).[95] The authors reported an outstanding increase in the adsorption capacity after the introduction of the MoS_2 in MXene. An excellent adsorption

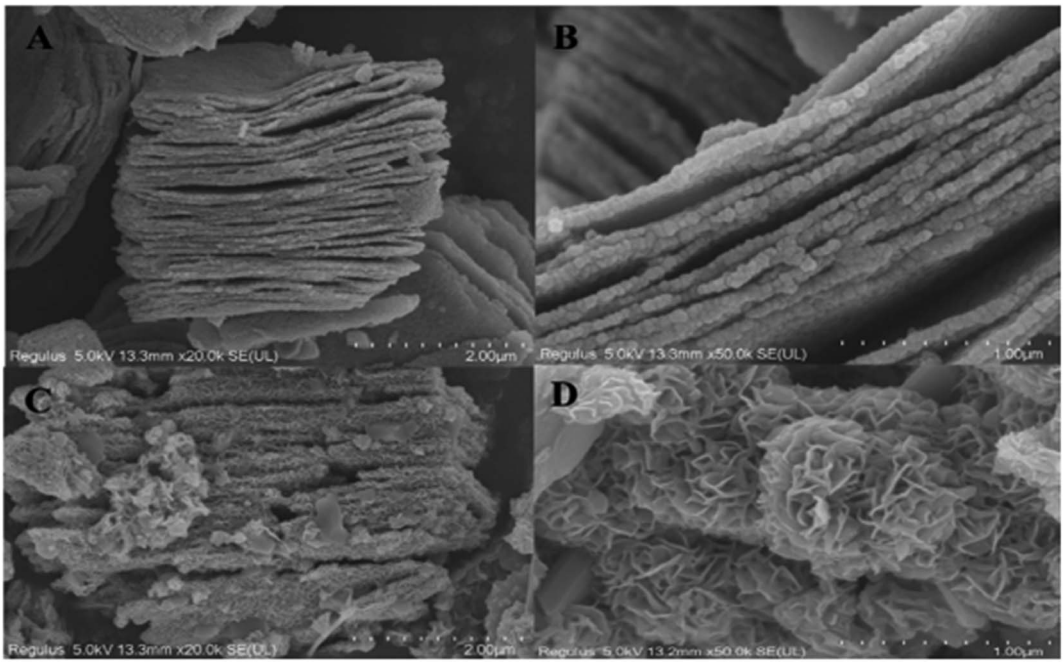

Fig. 8 SEM images of pure Ti_3C_2 (A and B) and MoS_2–Ti_3C_2 (C and D).[95]

capacity of 105.53 mg g^{-1} could be achieved within 30 min. Flower-like MoS_2 provided a greater number of adsorption sites and significantly increased the surface area of the prepared hybrid. The SEM images of flower-like MoS_2@MXene are illustrated in Fig. 8.[95]

Endocrine disruptor chemicals (EDC) are "an exogenous substance, or mixture of chemicals, that interferes with any part of hormone activity," according to the Endocrine Society. In other terms, Endocrine Disruptor Chemicals (EDCs) are chemicals that have the potential to negatively impact the endocrine system.[96] Most endocrine disrupting substances (EDS) and suspected EDCs are man-made and present in a variety of materials. These substances frequently bind to endogenous receptors, such as the oestrogen and steroid receptors, interfering with normal brain, reproductive, developmental, immunological, and another organ function.[97] People are exposed to EDCs in a variety of ways since they come from numerous sources, including the air that we breathe, the food we consume, and the water we drink. Skin contact is another way that EDCs can enter the body. Endocrine disruptor chemicals (EDC) are unavoidable harmful pollutants that are typically present in wastewater effluents that have been released, harming natural water bodies. This can be explained by the inefficient analytical techniques that prevent the development of wastewater treatment systems that could entirely mineralize the EDC by failing to quantify EDC in the treated wastewaters. Therefore, Rozaini and the research group fabricated a novel apparatus for micro-solid-phase extraction (μ-SPE) using an MXene-based adsorbent protected by polypropylene membrane for the adsorption of triclosan, triclocarban, 2-phenylphenol, bisphenol A and 4-*tert*-octylphenol from water samples.[98] When 2 mg of sorbent was applied, the maximum EDC extraction efficiency were attained. Indeed, MXene's hydrophilic characteristics were a result of the existence of O and F components. Therefore, it was proposed that for the extraction-cum-adsorption to occur, hydrogen bonds and a dipole–dipole interaction have to be created between the O or F in MXene and the electropositive sites from the EDC.

Phenolic compounds are toxic organic pollutants which are hazardous to both humans and the environment. An "oxidation-resistant MXene/poly(*N*-isopropylacrylamide) (PNIPAM) hydrogel thermosensitive" smart adsorbent with excellent adsorption efficiency and no secondary pollution features was designed to prevent phenol contamination by Wang *et al.*[99] The hydrogel adsorbent demonstrated exceptional oxidation resistance, and no noticeable alterations in structure and physicochemical properties were found even after 500 h of swelling in water. When the prepared smart adsorbent is subjected to the adsorption of 4-nitrophenol (4NP), a maximum adsorption capacity of 162 mg g^{-1} could be achieved. Furthermore, "MXene/PNIPAM and MXene–CTES–COOH/PNIPAM hydrogels" could only adsorb 141 and 136 mg g^{-1} of 4NP under similar

Table 1 Comparison of physicochemical parameters, experimental conditions, and adsorption capacities of various MXenes and MXene-supported adsorbents for the removal of organic contaminants

Organic contaminants	MXenes and MXenes-based adsorbents	Experimental conditions				Adsorption capacity (mg g^{-1})	Kinetics	Isotherms	References
		Initial conc. (mg L^{-1})	pH	Time (h)	Temp (°C)				
Methylene blue	$Ti_3C_2T_x$	50		20		39	—	Freundlich	30
Methylene blue	$Ti_3C_2T_x$	10	3.5–9.5	0–24	20–40	140	Pseudo-second order	Freundlich	72
Methylene blue	*h*-Ti_3C_2	50		2		24	—	—	75
Methylene blue	$Ti_3C_2T_x$	—	6–6.5		25	100	—	Langmuir	74
	LiOH–$Ti_3C_2T_x$					121			
	NaOH–$Ti_3C_2T_x$		8.8–9			189			
	KOH–$Ti_3C_2T_x$		8.8–9			77			
Methylene blue	Ti_3C_2–SO_3H	25–250	7	1.17	25	111.11	Pseudo-first order	Langmuir	78
MB	MXene	10	—	—	25	87	Pseudo-second-order model	Langmuir	76
	MXene–COOH					71			
	MXene–COOH@$(PEI/PAA)_{10}$					82			
MB	$Ti_3C_2T_x$ MXene bound with terephthalate	100	pH 7	6	20	209	Pseudo-second order	—	77
Amitriptyline	Sonicated $Ti_3C_2T_x$ MXene	0–22.2	7.0	—	—	241	—	—	61
Ciprofloxacin	Sodium intercalated $Ti_3C_2T_x$ MXene	1–300	5.5	2	25	208.2	Pseudo-second-order and Elovich	Redlich Peterson	63
Tetracycline	alk-MXene	50	5.5 ± 0.1	0.17	10, 25, and 40	7.16	—	Freundlich	65
Paraquat	Ti_3C_2–MoS_2 composites	20–200	3–10	—	28–90	165.38	Quasi-second-order	Freundlich isotherm	95
4-Nitrophenol	MXene-CTES-β-CD/PNIPAM nanocomposite hydrogels	400–2000	7	48	25–45	162	Pseudo-second order	Freundlich	99

conditions, illustrating the high stability, resistivity and outstanding adsorption capacity of MXene/poly(*N*-isopropylacrylamide). Also, it maintained 82% of its initial adsorption capacity after five adsorption cycles signifying a potential adsorbent for sewage treatment.[99]

$Ti_3C_2T_x$ was produced by Meng *et al.*[100] using the *in situ* LiF/HCl method. They used $Ti_3C_2T_x$ as an adsorbent to remove residue from the dialysis machine and urea from the aqueous wastewater. According to their research, $Ti_3C_2T_x$ had a lower adsorption capability of 10 mg g^{-1} at room temperature. Nevertheless, a 2.18-fold greater adsorption capacity (21.8 mg g^{-1}) was observed when the reaction temperature was raised to 37 °C. The urea molecules can be easily trapped between the MXene layers, according to the adsorption mechanism, and formed hydrogen bonds with the surface terminated functional groups. The findings demonstrate that the MXenes might be used as biocompatible adsorbents for efficient urea removal from an aqueous solution. According to Wu *et al.*[101] the $Ti_3C_2T_x$ has exceptional adsorption potential (88.2 mmol g^{-1}) against phenol molecules and followed the Langmuir and pseudo-first-order models. The recycling findings displayed superior reproducibility and long-lasting sustainability. Table 1 lists the physicochemical parameters, experimental conditions, and adsorption capacities of various MXenes and MXene-supported adsorbents for the removal of organic contaminants.

3.4. Heavy metals

Heavy metals should be eliminated from the water since they are dangerous even at very low quantities. Although there are several ways to get rid of metals, adsorption has been extremely effective. Because even at extremely low metal concentrations, the adsorption process is incredibly straightforward, affordable, and efficient. The removal of heavy metal ions from water and wastewater using novel MXene-based nanocomposites has been found to be extremely effective.

Various methods were used to modify the properties of MXenes and improve their efficacy in metal adsorption applications. For instance, in order to remove toxic Cr(VI), Ying *et al.*[102] prepared $Ti_3C_2T_x$ nanosheets using various HF acid concentrations (50, 25, and 10% weight percent). In comparison to $Ti_3C_2T_x$-25% (120 mg g^{-1}) and $Ti_3C_2T_x$-50% (170 mg g^{-1}), the $Ti_3C_2T_x$-10% showed a higher reductive removal capacity of Cr(VI) (250 mg g^{-1}). This was attributed to: (i) the $Ti_3C_2T_x$-10% nanosheets having larger inter-layer distances from XRD analysis than the $Ti_3C_2T_x$-25% and $Ti_3C_2T_x$-50% nanosheets, indicating that the intercalation and delamination processes are better suited to a low concentration of etchant solution; and (ii) the $Ti_3C_2T_x$-10% having the highest specific surface area of 57 m^2 g^{-1}. More crucially, the remaining Cr(VI) in treated water was significantly below the standard for drinking water advised by the WHO. Cr(VI) can be efficiently converted to less harmful Cr(III) species. At pH 5.0, the resultant Cr(III) can also be eliminated even without alkali treatment. The optimal circumstances are found at pH 5, which has the highest Cr(VI) and Cr(III) elimination performance. These $Ti_3C_2T_x$ nanosheets are potential candidates for removing harmful higher valent metal ion associated oxidants from water and wastewater due to their large surface area, good dispersibility, and reductivity.

In a different study, Tang and his team of researchers[103] demonstrated how MXenes flakes, which are produced by submerging Ti_3AlC_2 in HF solutions, can be utilised to remove Cr(VI) from water with a "adsorption capability of 80 mg g^{-1}." The stable high adsorption capacity may be explained by the functionalization and ample active sites present in the MXenes flakes.

Additionally, 2D MXenes were researched for the remediation of Cr(VI) and found to have a high adsorption capability of 104 mg g^{-1}.[104] The MXenes' uptake of Cr(VI) was predominantly caused by chemical sorption, particularly electrostatic adsorption, complex formation, ion exchange, and surface interactions. Additionally, it was evident from XPS and FTIR investigations that Cr(VI) was transferred into the interlayer of MXenes and adsorbed on their surface. A 0.1 M NaOH aqueous solution could also be used to successfully regenerate MXenes, and the removal efficiency was only marginally affected by the integrity loss and reactive functional groups. MXenes is an effective and selective adsorbent for removing Cr(VI) from aqueous solutions due to its great adsorption and removal efficiency.[104] Significant potential for the removal of Cr(VI) from water and wastewater was demonstrated by amino functionalized MXenes (NH_2–$Ti_3C_2T_x$).[105] $Ti_3C_2T_x$ sheets and amino moieties work together in a synergistic way to adsorb and reduce Cr(VI). The maximum Cr(VI) adsorption capacity of the NH_2–$Ti_3C_2T_x$ was 107.4 mg g^{-1}. NH_3^+ and Ti(II) are converted into NO_3^- and Ti(IV), respectively, with the removal of Cr(VI). Excellent selectivity and reusability were shown using MXene sheets with amino functionalization. The binding energy of Cr(VI) and electron density of the MXene surface are significantly increased by the synergistic interactions between Ti and N species.[105]

Several researchers have reported using MXenes-based nanocomposites to remove mercury (Hg) ions from water and wastewater. In this connection, $Ti_3C_2O_x$ MXene, which has a multifunctional adsorption performance of 4806 mg g^{-1}, was utilised by Fu and colleagues to remove Hg(II).[106] The combination of catalytic reduction and adsorption accounts for the good Hg(II) removal. The synthesised MXene demonstrated a variety of Hg(II) removal characteristics, including very fast adsorption kinetics, high selectivity and adsorption capacity, excellent recyclability, and efficiency over a wide range of pH. The synthesised MXene is a superior adsorbent for quick adsorption and extraction of Hg(II) from aqueous solution due to these characteristics.

The easy hydrothermal method used to successfully create the extremely stable magnetic titanium carbide based MXene nanocomposite (MGMX nanocomposite) and examined its ability to remove mercuric ions from water.[107] The synthesized MGMX nanocomposite displayed high stability as evidenced by zeta-potential measurement and dynamic light-scattering techniques. The MGMX nanocomposite showed good Hg(II) removal in a range of pH conditions, and an exceptional maximum experimental Hg(II) adsorption capacity of 1128.41 mg g^{-1} was reported. The MGMX nanocomposite used

in the adsorption/desorption investigation might be used up to five times.

In order to remove harmful mercuric ions, Hg(II), a novel "heterogeneous nanoadsorbent made of two-dimensional $Ti_3C_2T_x$ MXene nanosheets (MX) functionalized with nano-layered molybdenum disulfide (MoS_2/MX-II)" was developed.[108] The MoS_2-MX-II composite's sulphur (disulfide) and oxygenated terminal groups of $Ti_3C_2T_x$ worked together to effectively adsorb mercury. The $Ti_3C_2T_x$ nanosheets' surface area and interlayer distance rose during ultrasonication, improving the composite's capacity for removal. This led to a reduction of 50 mol L^{-1} of Hg(II) to 0.01 mol L^{-1} in under 120 seconds, which is an unusual kinetic behaviour for mercury adsorption. Additionally, the Langmuir adsorption isotherm additionally demonstrated a higher adsorption capability of 7.16 mmol g^{-1} and satisfactorily fitted the adsorption data. While applied to wastewater containing mercury, MoS_2/MX-II was able to remove Hg(II) at the parts per billion (ppb) level with a distribution coefficient of 7.87×10^5 mL g^{-1} even when other metal ions were present. It provided as a practical demonstration of the technology. After adsorbing a significant amount of Hg(II), the stability of MoS_2-MX-IIs was confirmed by hydrothermal stability measurement and SEM analysis. Additionally, MoS_2-MX-II demonstrated exceptional recyclability because even after five cycles, 0.08 mM of Hg(II) was fully eliminated. The outcomes point to the potential use of this kind of heterogeneous nanocomposite in the purification of water. Shahzad and colleagues[109] have created a new Ti_3CNT_x through the exfoliation of Ti_3AlC_2 MAX phases. The produced MXene adsorbent showed excellent adsorption of Hg(II) from water with an adsorption ability of 4606.04 mg g^{-1}. The co-ordination of –OH groups and bimetal with Hg(II) through adsorption-coupled reduction and electrostatic attraction accounts for their adsorption behaviour. With an exceptional dispersion coefficient of 1.36×10^9, the produced adsorbent displayed quicker kinetics.

Peng and his research teams[110] developed 2D alk-MXene ($Ti_3C_2(OH/ONa)_xF_{2-x}$) by chemical exfoliation coupled alkalization intercalation and investigated their ability to remove Pb(II) from aqueous phase in order to deal with lead pollution. According to reports, the adsorbent demonstrated greater adsorption capabilities of 140 mg g^{-1}. The produced alk-MXene displayed a number of remarkable qualities, including higher sorption capacity, quicker kinetics, reversible characteristics, and the ability to address extremely low Pb concertation (II). Dong *et al.*[111] examined the adsorption potential of Pb(II) using an MXene/alginate composite, and discovered that it had an adsorption capacity of 382.7 mg g^{-1}. Chemical co-ordination and ion exchange are proposed as the adsorption mechanism by the authors. In a different study, MXene is functionalized with an amino group and used to remove Pb(II) from water.[111] The authors reported that the adsorption potential was 384.63 mg g^{-1}. Their increased adsorption capacity, according to them, is mostly due to amine and hydroxyl surface complexation.

Ba(II) and Cu(II) ions, two common water contaminants, are also effectively adsorbed by $Ti_3C_2T_x$ MXene. It is discovered that the Ba(II) ion adsorption procedure benefits from the creation of both Ba–O and Ba–F bonds.[112] Fard *et al.*[113] showed that the highest adsorption capacity is 9.3 mg g^{-1} for an initial barium concentration of 55 ppm using novel 2-D MXene nanosheets ($Ti_3C_2T_x$), which is greater than that of activated carbon and carbon nanotubes. Additionally, under ideal circumstances, removal efficiency can reach up to 100% under optimal conditions. More thorough research may be required to fully understand the effects of –F groups on adsorption system because other studies[110] claimed that –F groups prevent the adsorption

Table 2 Comparison of experimental conditions, physicochemical parameters, and adsorption capacity of heavy metals using various MXenes and MXenes-supported adsorbents

MXenes and MXenes-based adsorbents	Metals	Experimental conditions: Initial conc. (mg L^{-1})	pH	Temp. (°C)	Adsorption capacity (mg g^{-1})	Kinetics	Isotherms	References
2-D alk-MXene ($Ti_3C_2(OH/ONa)_xF_{2-x}$)	Pb(II)	10–300	1–7	20–52	140	—	—	108
2D-$Ti_3C_2T_x$ MXenes	Cr(VI)	100	3	30	104	Pseudo-first-order	Langmuir	104
Amino-functionalized MXenes (NH_2–$Ti_3C_2T_x$)	Cr(VI)	100	2–9	25–70	107.4	Pseudo-second-order model	Langmuir	105
Multilayered oxygen-functionalized Ti_3C_2 ($Ti_3C_2O_x$) nanosheets	Hg(II)	10–1000	3–12	25	4806	—	Langmuir	104
Magnetic titanium carbide ($Ti_3C_2T_x$) MXene nanocomposite	Hg(II)	10	6	25	1128.41	Pseudo second-order	Redlich–Peterson	107
Molybdenum disulfide-functionalized MXene nanocomposites (MoS_2–MX-II composites)	Hg(II)	0.05 mmol L^{-1}	6.5	25	1435.20	Pseudo second-order	Langmuir	108
2D alk-MXene ($Ti_3C_2(OH/ONa)_xF_{2-x}$)	Pb(II)	50	1–7	20–50	140.1	—	—	104
Amino-functionalized $Ti_3C_2T_x$MXene (alk-MXene-NH_2) nanosheets	Pb(II)	500	1.0–6.3	25–45	384.63	Pseudo second-order	Langmuir	110
MXene/alginate composites	Pb(II)	1.5 mM	1–7	25–60	382.7	Pseudo-second-order	Langmuir	109
MXene/alginate composites	Cu(II)	1.5 mM	1–7	25–60	87.6	Pseudo-second-order	Langmuir	109

of metal ions. In addition, the prepared 2-D MXene nanosheets ($Ti_3C_2T_x$) demonstrated large adsorption capacity, rapid kinetics, removal of enormous detectable barium, and reversible adsorption properties.[113] MXene's ability to completely remove barium before injecting sea water as required by industry was demonstrated by its removal efficacy of barium and leftover barium in co-produced water. Investigations on MXene's performance in multi-metal solutions revealed that it had a very high selectivity for removing barium when compared to certain other coexisting metals in the solution.[111] Zhang *et al.*[114] used functionalized 2-Dimensional $Ti_3C_2T_x$ (TN-EHL) for effective removal of Cu(II) from water. The $Ti_3C_2T_x$ nanosheets were functionalized with enzymatic hydrolysis lignin (EHL). EHL can prevent $Ti_3C_2T_x$ from oxidising in addition to providing reactive functional groups to TN-EHL, which enhances the adsorption capacity of TN-EHL. The maximum adsorption capacity of TN-EHL50, which contains 50% EHL, was reported as 49.96 mg g^{-1}. The thermodynamic investigation shows that Cu(II) adsorption on TN-EHL50 is spontaneous and endothermic in nature. In the adsorption process, Cu(II) ions were dramatically reduced to Cu_2O and CuO. TN-EHL seems to have a great potential for the adsorptive removal of Cu(II). To sum up, both pure and functionalized MXenes demonstrated efficient heavy metal removal. The versatility of their surface chemistry, the variety of functional groups, and their capacity to respond to localized chemical and electrical disturbance are all factors that contribute to the MXene-based adsorbents' efficiency. These factors give them a distinctive reductive adsorptive behaviour. Table 2 showed the experimental conditions, physicochemical parameters, and adsorption capacity of heavy metals using various MXenes and MXenes-supported adsorbents.

4. Adsorption mechanism of organic contaminants and metals on MXenes

It's critical to comprehend the adsorption mechanisms and interactions between pollutants and adsorbents because MXene-based adsorbents have the ability to adsorb a variety of environmental pollutants because of their distinctive architectures.[102] To get a sense of the precise likely uptake mechanism, various spectroscopic techniques, adsorption isotherms and kinetics, and theoretical simulations using density functional theory must be carried out. The interaction of organic contaminants with the functional groups of MXenes primarily leads to contaminants adsorption on the materials. However, physical characteristics, including hydrate diameter and kinetics of agglomeration, were also believed to have substantially affected the system's adsorption performance.[115,116] The charges on the adsorbent and the adsorbate are crucial because electrostatic interaction is the primary mechanism of adsorption regardless of whether the pollutant is an organic or an inorganic substance.[72,78,115] Water quality factors including pH, temperature, and the prevalence of background ions and natural organic matter (NOM) have a significant impact on the adsorption process of organic pollutants, just as they do on the elimination of inorganic pollutants. Although electrostatic interaction is the predominant mechanism for inorganic contaminants removal, other mechanisms, such as ion exchange, as well as some factors, such as specific surface area, pH, and temperature, also significantly influence the adsorption process.[99,107,110]

Fig. 9 depicts the AA2-alk-MXene adsorption mechanism diagram for MB and CR.[87] Three adsorption mechanisms may be primarily involved in the adsorption of the two dyes:

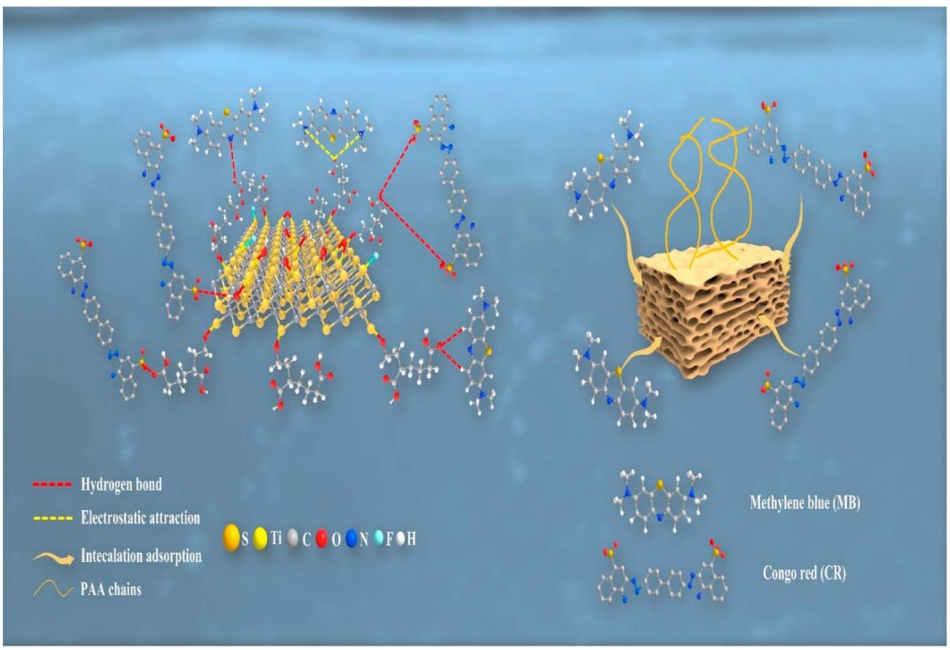

Fig. 9 Graphical representation of adsorption mechanism of AA2-alk-MXene on MB and CR.[87]

hydrogen bonding is depicted by the red dotted line (a). The most frequent type of interaction force is a hydrogen bond, which is primarily produced by the union of hydroxyl groups on the AAX-alk-MXene lamellae surface and –COOH groups on the long chain of PAA with nitrogen atoms from MB, nitrogen atoms from CR, and sulfonates.[49,75] Electrostatic adsorption is indicated by the yellow dotted line (b). The primary source of this adsorption mechanism is the electrostatic interaction between the nitrogen atoms on methylene blue and –COOH groups on PAA long chain of AAX-alk-MXene.[23] The yellow arrow, meanwhile, denotes intercalation adsorption (c). The AAX-alk-MXene lamellae's slit pores serve as the key support for this mechanism. The AAX-alk-MXene adsorption mechanisms for CR are hydrogen bonds and intercalation adsorption; for MB, the mechanisms are electrostatic interactions and intercalation adsorption. The surface of CR has a higher concentration of oxygen-containing functional groups, resulting in a stronger H-bonding with the adsorbents. According to the TGA and XPS investigations, the injection of acrylic acid, which is a relatively small amount, has a significant impact on the adsorption behaviour of methylene blue. This explains why AA-alk-MXene has a higher adsorption capability for CR than MB.

The proposed mechanism for the adsorption of methylene blue on the V_2CT_x MXene surface was demonstrated in Fig. 10.[117] According per the opinion of the authors, the primary adsorption mechanism between methylene blue and MXene was identified as the electrostatic interactions. The MB^+ molecules can interact with the hydroxyl groups on the titanium surface to ionize H^+ and form a monodentate complex *via* the M–O–HN bond, as shown in eqn (1) and (2).

$$TiOH \leftrightarrows Ti\text{–}O^- + H^+ \quad (1)$$

$$Ti\text{–}O^- + MB^+ \leftrightarrows TiO - MB \quad (2)$$

The adsorption of MB facilitates the formation of the complex; however, the repulsion between the cationic dye and positively charged MXene@Fe_3O_4 hinders the formation of the complex. Furthermore, MB is probably reduced by $Ti_3C_2T_x$ nanosheets and then adsorbed onto the MXene@Fe_3O_4 surface due to interactions between the OH group and the Ti site. Additionally, dipole–dipole H-bonding between "N of MB and Ti–OH groups" result in the formation of the O–H–N bond. According to Li *et al.*[76] adsorption of MB onto MXene-COOH@$(PEI/PAA)_n$ core–shell nanocomposite is a three-step process that involves external surface adsorption; dispersion of particles internally, and the last step of attaining adsorption equilibrium. Adsorption followed by photocatalytic degradation causes the MXene ($Ti_3C_2T_x$) to remove the cationic dye MB from wastewater.[31] Here, the different steps of $Ti_3C_2T_x$'s MB removal are discussed. The dye molecules are first adsorbed on $Ti_3C_2T_x$, causing a rise in stacking disorder, possibly due to Mxene's chemical change and wedging of its layered structure. Titania is created as a result of the oxidation of MXene ($Ti_3C_2T_x$), which is the last step.

XPS was also used to investigate the adsorption mechanism between the compound hydrogel and 4-NP.[99] After 4-NP adsorption, the composite hydrogel's distinctive C 1s (correction), N 1s, and O 1s peaks dramatically increased, demonstrating that 4-NP was adsorbed. After 4-NP adsorption, the fitted C–O and C=O peaks in the composite hydrogel's C 1s spectra migrated to 286.31 and 287.62 eV, respectively. The C–O and C=O fitting peaks in the O 1s spectra shifted to 531.28 and 532.36 eV, respectively, indicating that the 4-NP, carbonyl, and

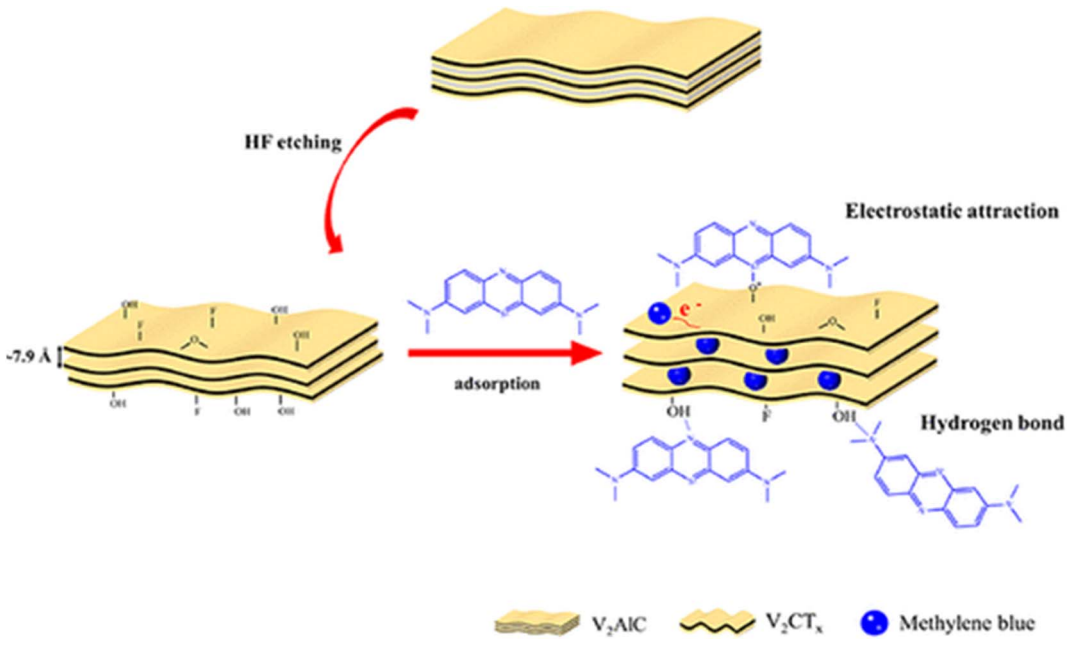

Fig. 10 Mechanism of adsorption of MB on V_2CTx MXene surface.[117]

hydroxyl formed hydrogen bonds during the adsorption process.

The numerous reaction sites and surface functional groups of novel nanomaterials would facilitate the effective removal of heavy metal ions. Chelation, chemisorption, chemical coordination, diffusion, electrostatic interactions, ion exchange, surface complexation, and van der Waals interactions are some of the often-described mechanisms of removing harmful heavy metal ions from water. Ying *et al.*[102] investigated the Cr(VI) adsorption mechanism by the $Ti_3C_2T_x$ nanosheets. The main processes include reducing Cr(VI) to Cr(III), precipitating $Cr(OH)_3$ at pH > 4.8, and electrostatic attraction between the adsorbent surface and the negatively charged $Cr_2O_7^{-2}$ in an acidic environment.[102]

5. Reusability of MXene-based nanocomposite adsorbents

Before adopting MXene for actual application, it is crucial to examine its capacity for recurrent dye adsorption on MXene and MXene-based composites to lower the replacement cost in treatment of wastewater. Numerous studies have demonstrated the extraordinary stability of MXenes and MXene-based nanocomposites and their potential for regeneration and recycling after dye adsorption. The stability and recyclability of MXene@Fe_3O_4 are examined for five repetitions of the adsorption–desorption cycles for MB removal by Zhang *et al.*[118] The MXene@Fe_3O_4 was treated with ethanol, collected using a magnet, and dried at 70 °C after the adsorption of MB.[118] Comparing the removal efficiencies across various recycle runs reveals that MXene@Fe_3O_4 exhibits a little decline in the removal efficacy toward MB, which maintained at around 77% after five cycles of operation. The operating parameters include a 1 g L^{-1} MXene@Fe_3O_4 dose, a 24 h reaction time, and a 10 mg L^{-1} initial concentration of MB. The obtained data shows that MXene@Fe_3O_4 composites can function as an extremely reliable and recyclable adsorbent for the removal of methylene blue.[118]

Li *et al.*[76] showed that MXeneCOOH@$(PEI/PAA)_n$ can be reused for up to 8 cycles with a negligible decrease in adsorption capacity due to regeneration after MB adsorption. The fabrication of recyclable, high-performance and cost-effective adsorbents largely depends on adsorbent recycling. Investigations on the regeneration of MXene-supported adsorbents have been conducted using various basic, acidic, and salt-based regeneration solutions. The selection of regeneration agents is influenced by the frequency of adsorption–desorption cycles, the effectiveness of desorption, and stability of the adsorbent. The most prominent regeneration agents for MXene-supported adsorbents include HNO_3, HCl, and $Ca(NO_3)_2$. Other substances, such as $SC(NH_2)_2$, Na_2EDTA, and NaOH, were also used. The most often utilised desorption agent for recycling used adsorbents among acidic reagents is HCl solution.[119] Jun *et al.*[115] investigated the removal of MB using MXene during the regeneration tests. The MB removing recyclability of MXene after the fourth cycle of operation is shown in Fig. 11. After the fourth cycle, MXenes had somewhat decreased removal rates; this might be because the adsorbents couldn't be fully recovered by physical separation because the N 1s peak of MXene completely disappeared after washing. Mxene adsorbents still had a Q_e of more than 50 mg g^{-1} after four cycles of operation, showing that they can be used as practical and affordable adsorbents for dye-containing wastewater treatment.

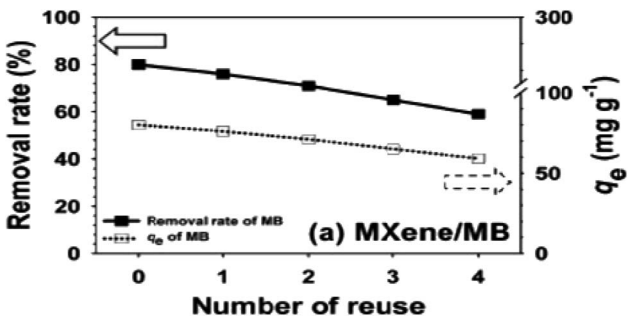

Fig. 11 Reusability performance of MXene's for the adsorption of MB.[115]

Most of these experiments have demonstrated that MXene adsorbent materials perform effectively during renewal. Additionally, stability, which could be a significant issue with MXenes, has not yet been well investigated. The oxidation of MXene surfaces to rutile TiO_2 particles may lead to the loss of functional groups present on the surface, and a decrease in the number of available active sites has been shown in many studies to cause the $Ti_3C_2T_x$ MXene solution's colour to change from black to grey during the adsorption.[120–122] Even though the previous research on improved MXene has somewhat improved the permanence of some MXenes,[123,124] further research is still needed.

6. Limitations and future prospective

MXenes offer considerable benefits over conventional sorbents, such as carbon and graphene-based materials, in terms of customizable surface chemistry and strong hydrophilicity, facilitating the surface absorption of various contaminants. 2-D transition metal carbides/nitrides, or MXenes, have shown highly promising outcomes in the adsorption of diverse contaminants, such as heavy metal ions, organic dyes, pharmaceuticals and other pollutants. Overall, they appear to perform better than other 2-D materials like carbon nanotubes and graphene as well as other traditional adsorbents.

Due to their distinct characteristics, 2-dimensional nanomaterials are more selective and have a higher adsorptive capacity than other dimensional materials. However, because two-dimensional nanomaterials are frequently widely distributed in water, it is difficult to recycle 2-D nanomaterials from water after adsorption. Secondary contamination can possible when separation is insufficient. Additionally, the expense and lower yield of 2-D nanomaterials prevent their industrial-scale manufacture. Several 2-dimensional nanomaterials, particularly 2-dimensional MOFs, demonstrate poor stability in water. Practical applications are greatly constrained by the absence of

aqueous stability. Future research should focus on improving the water stability of 2-D nanomaterials for usage in aquatic environments.

MXenes are unstable (*i.e.*, under CO_2, air, and other environments), especially Ti_3C_2, which has been reported to be the most effective for treating water. However, this instability can be overcome by modifying MXenes with glucose, dopamine, hyaluronic acid, or polyethylene glycol (PEG) to increase durability.[125] Ta_4C_3 was superficially changed with soybean phospholipids, while Nb_2C was modified with polyvinylpyrrolidone (PVP).[126] Notably, just a small number of MXenes were employed for wastewater treatment, so it is crucial to make use of further MXenes to understand the structural–performance relationship and to ascertain the materials' dependability, longevity, and post-treatment procedures.[127] The biocompatibility of MXenes can be improved through surface modification, which also decreases their cytotoxic impact on aquatic habitats and biota.

To safely develop and dispose of MXene-containing materials, more research is required to investigate the toxicity of MXenes on living creatures. The implementation of MXenes in industrial-scale and commercial water treatment applications is constrained by practical problems with the large-scale synthesis of MXenes absorbents. MXenes cannot be scaled up for usage in practical water treatment applications since the synthesis process is currently challenging and involves numerous reaction stages, dangerous chemicals, lower production yield, and specific safety considerations.

In order to help with practical water treatment, it is essential to develop easy, superficial, and one-step synthesis techniques because, despite significant progressions in MXene fabrication process, there is a serious flaw in the synthesis method. When creating MXene and MXene-based nanocomposites, it's really a good idea to consider substituting toxic HF with some eco-friendly compounds. In order to enhance the adsorptive removal of organic contaminants and heavy metals, additional morphological features with different morphologies and characteristic properties should be discussed.

Furthermore, it is important to investigate the stability of MXenes to permit a workable wastewater remediation process. Additionally, it has not yet been reported how to create MXenes that are successful in removing a mixture of dyes at different pH conditions. Due to their unique physiochemical advantages, modified carbon compounds can considerably increase the dye adsorption capacities of MXenes.[128–131] The disparity between theoretically predicted accuracy and actual applications of MXenes must be addressed for a better understanding of composition and structure of MXenes. Further experimental efforts must be made to synthesize various new types of MXenes for dye removal. More research should be done to investigate the adsorption of various other organic compounds other than dyes like cosmetics, pharmaceuticals, pesticides, *etc.*

It is still a need to research low-molecular-weight MXenes like Ti_2CT_x. Despite the widely reported achievements of higher molecular weight MXenes ($Ti_3C_2T_x$) in the treatment of wastewater, more research on the clusters of MXenes should be done to enhance the application of MXenes in wastewater treatment. Analysis of the stability and adsorption mechanisms of MXene should be the main focus of future study. As a result, using MXenes in environmental applications could be scaled up more easily. There are no investigations on continuous flow fixed-bed column tests for the elimination of contaminants utilising MXene and MXene-based nanocomposites because all of the aforementioned research is focused on lab-scale batch experiments. There should be more focus on scaling up the research with predicting material costs and financial viability. The efficiency of "MXene adsorbents" in artificial wastewater containing different ions has not been extensively studied.

Therefore, it is necessary to research the effectiveness of MXenes in pilot wastewater treatment. The alteration to the surface MXene effectively improves MXene efficiency and reduces their negative effects on aquatic environments and lifeforms. Collagen-modified MXenes, such as Ti_3C_2 and Ti_2C, have shown lesser toxicity and superior cell survival in human skin malignant melanoma cells as compared to unmodified MXenes. Ti_3C_2 quantum dots were found to be more dangerous than Nb_2C at the same mass when tested on human umbilical vein endothelial cells.[132] More research into the cytotoxic effects of MXenes on living beings is necessary in order to safely develop and dispose substances containing MXene. Future research should examine how MXenes may affect the ecosystem. There hasn't been much discussion of the harmful effects of MXenes on both people and the environment. The production yield of MXenes is still low compared to previously used precursors, and its complicated fabrication process still necessitates numerous reaction steps, dangerous chemicals, and special safety precautions. As a result, MXenes cannot be upscaled for actual wastewater treatment applications.

7. Conclusion

This review emphasizes the current successes of MXenes as adsorbent material for adsorption of organic contaminants and heavy metals from water and wastewater. It has been demonstrated that MXenes are possible new generation materials for the removal of pharmaceuticals, heavy metals, and dyes, including methylene blue, methyl orange, rhodamine B, *etc.*, from aqueous streams.

The electrostatic attraction between the oxygen-containing functional groups on MXenes and organic contaminants is responsible for their adsorption. The pH and temperature being extensively examined for organic contaminants sorption generally affect the rate of sorption. According to the desorption study, MXene is recyclable and can be renewed by washing in a weak aqueous acid. MXene may be a promising material for applications involving the removal of organic contaminants and heavy metals from water and environmental protection due to its high reusability and sorption effectiveness. However, more study is required to create an effective synthesis method for the mass manufacture of new nanocomposites based on MXene. The adsorption of organic contaminants and heavy metals on MXene-based nanocomposites is influenced by several variables, including solution pH, temperature, ionic strength, *etc.* Reduced starting concentration, increased temperature,

increased adsorbent dosage and increased contact time all increase the adsorption efficiency. However, each organic contaminants and metals favour different physical and chemical conditions for adsorption. It is concluded that MXene-based nanocomposites may be an excellent material for the removal of organic contaminants and heavy metals from water and wastewater.

Conflicts of interest

There are no conflicts to declare.

References

1 W. J. Cosgrove and D. P. Loucks, Water management: current and future challenges and research directions, *Water Resour. Res.*, 2015, **51**(6), 4823–4839.
2 M. Ahmaruzzaman, Nano-materials: novel and promising adsorbents for water treatment, *Asian J. Water, Environ. Pollut.*, 2019, **16**(3), 43–53.
3 M. J. K. Ahmed, M. Ahmaruzzaman and R. A. Reza, Lignocellulosic-derived modified agricultural waste: development, characterization and implementation in sequestering pyridine from aqueous solutions, *J. Colloid Interface Sci.*, 2014, **428**, 222–234.
4 M. Ahmaruzzaman, D. Mohanta and A. Nath, Environmentally benign fabrication of SnO_2-CNT nanohybrids and their multifunctional efficiency as an adsorbent, catalyst and antimicrobial agent for water decontamination, *Sci. Rep.*, 2019, **9**(1), 1–19.
5 M. Abhinaya, R. Parthiban, P. S. Kumar and D. V. N. Vo, A review on cleaner strategies for extraction of chitosan and its application in toxic pollutant removal, *Environ. Res.*, 2021, **196**, 110996.
6 M. Ahmaruzzaman and D. K. Sharma, Adsorption of phenols from wastewater, *J. Colloid Interface Sci.*, 2005, **287**, 14–24, DOI: **10.1016/J.JCIS.2005.01.075**.
7 M. Ahmaruzzaman, Industrial wastes as low-cost potential adsorbents for the treatment of wastewater laden with heavy metals, *Adv. Colloid Interface Sci.*, 2011, **166**, 36–59, DOI: **10.1016/J.CIS.2011.04.005**.
8 M. J. K. Ahmed and M. Ahmaruzzaman, A review on potential usage of industrial waste materials for binding heavy metal ions from aqueous solutions, *J. Water Process. Eng.*, 2016, **10**, 39–47, DOI: **10.1016/J.JWPE.2016.01.014**.
9 S. A. Khan, N. Abbasi, D. Hussain and T. A. Khan, Sustainable mitigation of paracetamol with a novel dual-functionalized pullulan/kaolin hydrogel nanocomposite from simulated wastewater, *Langmuir*, 2022, **38**(27), 8280–8295.
10 S. A. Khan, D. Hussain, N. Abbasi and T. A. Khan, Deciphering the adsorption potential of a functionalized green hydrogel nanocomposite for aspartame from aqueous phase, *Chemosphere*, 2022, **289**, 133232.
11 Y. Fan, L. Li, Y. Zhang, X. Zhang, D. Geng and W. Hu, Recent advances in growth of transition metal carbides and nitrides (MXenes) crystals, *Adv. Funct. Mater.*, 2022, **32**(16), 2111357.
12 M. Naguib, M. Kurtoglu, V. Presser, J. Lu, J. Niu, M. Heon, L. Hultman, Y. Gogotsi and M. W. Barsoum, Two-dimensional nanocrystals produced by exfoliation of Ti_3AlC_2, *Adv. Mater.*, 2011, **23**, 4248–4253, DOI: **10.1002/adma.201102306**.
13 M. Naguib and Y. Gogotsi, Synthesis of two-dimensional materials by selective extraction, *Acc. Chem. Res.*, 2015, **48**, 128–135, DOI: **10.1021/ar500346b**.
14 M. W. Barsoum, The MN+1AXN phases: a new class of solids: thermodynamically stable nanolaminates, *Prog. Solid State Chem.*, 2000, **28**, 201–281, DOI: **10.1016/S0079-6786(00)00006-6**.
15 Z. Sun, D. Music, R. Ahuja, S. Li and J. M. Schneider, Bonding and classification of nanolayered ternary carbides, *Phys. Rev. B: Condens. Matter Mater. Phys.*, 2004, **70**, 092102, DOI: **10.1103/PhysRevB.70.092102**.
16 M. Naguib, V. N. Mochalin, M. W. Barsoum and Y. Gogotsi, 25th anniversary article: MXenes: a new family of two-dimensional materials, *Adv. Mater.*, 2014, **26**, 992–1005, DOI: **10.1002/adma.201304138**.
17 R. Garg, A. Agarwal and M. Agarwal, A review on MXene for energy storage application: effect of interlayer distance, *Mater. Res. Express*, 2020, **7**, 022001, DOI: **10.1088/2053-1591/AB750D**.
18 H. Tang, Q. Hu, M. Zheng, Y. Chi, X. Qin, H. Pang and Q. Xu, MXene–2D layered electrode materials for energy storage, *Prog. Nat. Sci.: Mater. Int.*, 2018, **28**, 133–147, DOI: **10.1016/J.PNSC.2018.03.003**.
19 A. Iqbal, P. Sambyal and C. M. Koo, 2D MXenes for Electromagnetic Shielding: A Review, *Adv. Funct. Mater.*, 2020, **30**, 2000883, DOI: **10.1002/ADFM.202000883**.
20 X. Jiang, A. V. Kuklin, A. Baev, Y. Ge, H. Ågren, H. Zhang and P. N. Prasad, Two-dimensional MXenes: From morphological to optical, electric, and magnetic properties and applications, *Phys. Rep.*, 2020, **848**, 1–58, DOI: **10.1016/J.PHYSREP.2019.12.006**.
21 J. C. Gui, L. Han and W. ying Cao, Lamellar MXene: A novel 2D nanomaterial for electrochemical sensors, *J. Appl. Electrochem.*, 2021, **51**, 1509–1522, DOI: **10.1007/S10800-021-01593-7**.
22 Q. Tao, M. Dahlqvist, J. Lu, S. Kota, R. Meshkian, J. Halim, J. Palisaitis, L. Hultman, M. W. Barsoum, P. O. Å. Persson and J. Rosen, Two-dimensional Mo1.33C MXene with divacancy ordering prepared from parent 3D laminate with in-plane chemical ordering, *Nat. Commun.*, 2017, 1–7, DOI: **10.1038/ncomms14949**.
23 H. Zhang, T. Hu, W. Sun, M. Hu, R. Cheng and X. Wang, Atomic Repartition in MXenes by Electron Probes, *Chem. Mater.*, 2019, **31**, 4385–4391, DOI: **10.1021/ACS.CHEMMATER.9B00470**.
24 M. B. Kanoun, S. Goumri-Said and K. Abdullah, Theoretical study of physical properties and oxygen incorporation effect in nanolaminated ternary carbides 211-MAX phases, *Adv. Sci. Technol.* $M_{n+1}AX_n$, 2012, 177–196, DOI: **10.1533/9780857096012.177**.

25 Y. C. Zhou, X. H. Wang, Z. M. Sun and S. Q. Chen, Electronic and structural properties of the layered ternary carbide Ti_3AlC_2, *J. Mater. Chem.*, 2001, **11**, 2335–2339, DOI: 10.1039/B101520F.

26 J. C. Lei, X. Zhang and Z. Zhou, Recent advances in MXene: Preparation, properties, and applications, *Front. Phys.*, 2015, **10**, 276–286, DOI: 10.1007/S11467-015-0493-X.

27 F. Chang, C. Li, J. Yang, H. Tang and M. Xue, Synthesis of a new graphene-like transition metal carbide by de-intercalating Ti3AlC2, *Mater. Lett.*, 2013, **109**, 295–298, DOI: 10.1016/J.MATLET.2013.07.102.

28 V. M. H. Ng, H. Huang, K. Zhou, P. S. Lee, W. Que, J. Z. Xu and L. B. Kong, Recent progress in layered transition metal carbides and/or nitrides (MXenes) and their composites: synthesis and applications, *J. Mater. Chem. A*, 2017, **5**(7), 3039–3068, DOI: 10.1039/C6TA06772G.

29 J. Halim, M. R. Lukatskaya, K. M. Cook, J. Lu, C. R. Smith, L. Å. Näslund, S. J. May, L. Hultman, Y. Gogotsi, P. Eklund and M. W. Barsoum, Transparent conductive two-dimensional titanium carbide epitaxial thin films, *Chem. Mater.*, 2014, **26**, 2374–2381, DOI: 10.1021/CM500641A.

30 L. Wang, H. Zhang, B. Wang, C. Shen, C. Zhang, Q. Hu, A. Zhou and B. Liu, Synthesis and electrochemical performance of $Ti_3C_2T_x$ with hydrothermal process, *Electron. Mater. Lett.*, 2016, **125**, 702–710, DOI: 10.1007/S13391-016-6088-Z.

31 O. Mashtalir, K. M. Cook, V. N. Mochalin, M. Crowe, M. W. Barsoum and Y. Gogotsi, Dye adsorption and decomposition on two-dimensional titanium carbide in aqueous media, *J. Mater. Chem. A*, 2014, **2**, 14334–14338, DOI: 10.1039/C4TA02638A.

32 M. Ghidiu, M. Naguib, C. Shi, O. Mashtalir, L. M. Pan, B. Zhang, J. Yang, Y. Gogotsi, S. J. L. Billinge and M. W. Barsoum, Synthesis and characterization of two-dimensional Nb_4 C_3 (MXene), *Chem. Commun.*, 2014, **50**, 9517–9520, DOI: 10.1039/C4CC03366C.

33 K. A. Maleski, *Solution Processing and Optical Properties of 2D Transition Metal Carbides (MXenes)*, 2019, DOI: 10.17918/1q0w-rv44.

34 Y. U. Haq, R. Ullah, S. Mazhar, R. Khattak, A. A. Qarni, Z. U. Haq and S. Amin, Synthesis and characterization of 2D MXene: Device fabrication for humidity sensing, *J. Sci.: Adv. Mater. Devices*, 2022, 7(1), 100390.

35 E. Lee, A. VahidMohammadi, B. C. Prorok, Y. S. Yoon, M. Beidaghi and D. J. Kim, Room temperature gas sensing of two-dimensional titanium carbide (MXene), *ACS Appl. Mater. Interfaces*, 2017, **9**, 37184–37190, DOI: 10.1021/acsami.7b11055.

36 Q. Xue, H. Zhang, M. Zhu, Z. Pei, H. Li, Z. Wang, Y. Huang, Y. Huang, Q. Deng, J. Zhou, S. Du, Q. Huang and C. Zhi, Photoluminescent Ti_3 C_2 MXene quantum dots for multicolor cellular imaging, *Adv. Mater.*, 2017, 29, DOI: 10.1002/adma.201604847.

37 Y. Feng, H. Wang, J. Xu, X. Du, X. Cheng, Z. Du and H. Wang, Fabrication of MXene/PEI functionalized sodium alginate aerogel and its excellent adsorption behavior for Cr(VI) and Congo Red from aqueous solution, *J. Hazard. Mater.*, 2021, **416**, 125777.

38 C. Cui, R. Guo, E. Ren, H. Xiao, X. Lai, Q. Qin, S. Jiang, H. Shen, M. Zhou and W. Qin, Facile hydrothermal synthesis of rod-like Nb_2O_5/Nb_2CT_x composites for visible-light driven photocatalytic degradation of organic pollutants, *Environ. Res.*, 2021, **193**, 110587.

39 M. Shekhirev, C. E. Shuck, A. Sarycheva and Y. Gogotsi, Characterization of MXenes at every step, from their precursors to single flakes and assembled films, *Prog. Mater. Sci.*, 2021, **120**, 100757, DOI: 10.1016/J.PMATSCI.2020.100757.

40 X. Sheng, S. Li, H. Huang, Y. Zhao, Y. Chen, L. Zhang and D. Xie, Anticorrosive and UV-blocking waterborne polyurethane composite coating containing novel two-dimensional Ti_3C_2 MXene nanosheets, *J. Mater. Sci.*, 2021, **56**, 4212–4224, DOI: 10.1007/S10853-020-05525-2.

41 A. Caggiano, G. Granozzi, S. Biswas and P. S. Alegaonkar, MXene: Evolutions in Chemical Synthesis and Recent Advances in Applications, *Surfaces*, 2022, **5**, 1–34, DOI: 10.3390/SURFACES5010001.

42 F. Liu, A. Zhou, J. Chen, J. Jia, W. Zhou, L. Wang and Q. Hu, Preparation of Ti_3C_2 and Ti_2C MXenes by fluoride salts etching and methane adsorptive properties, *Appl. Surf. Sci.*, 2017, **416**, 781–789, DOI: 10.1016/J.APSUSC.2017.04.239.

43 T. Hu, M. Hu, Z. Li, H. Zhang, C. Zhang, J. Wang and X. Wang, Covalency-Dependent Vibrational Dynamics in Two-Dimensional Titanium Carbides, *J. Phys. Chem. A*, 2015, **119**, 12977–12984, DOI: 10.1021/ACS.JPCA.5B08626.

44 A. Champagne, L. Shi, T. Ouisse, B. Hackens and J. C. Charlier, Electronic and vibrational properties of V_2C-based MXenes: From experiments to first-principles modeling, *Phys. Rev. B.*, 2018, **97**, 115439, DOI: 10.1103/PHYSREVB.97.115439.

45 A. S. Levitt, M. Alhabeb, C. B. Hatter, A. Sarycheva, G. Dion and Y. Gogotsi, Electrospun MXene/carbon nanofibers as supercapacitor electrodes, *J. Mater. Chem. A*, 2018, **7**, 269–277, DOI: 10.1039/C8TA09810G.

46 J. Tang, T. S. Mathis, N. Kurra, A. Sarycheva, X. Xiao, M. N. Hedhili, Q. Jiang, H. N. Alshareef, B. Xu, F. Pan and Y. Gogotsi, Tuning the Electrochemical Performance of Titanium Carbide MXene by Controllable *In Situ* Anodic Oxidation, *Angew. Chem.*, 2019, **131**, 18013–18019, DOI: 10.1002/ANGE.201911604.

47 Y. Jin, Y. Fan, X. Meng, W. Zhang, B. Meng, N. Yang and S. Liu, Theoretical and Experimental Insights into the Mechanism for Gas Separation through Nanochannels in 2D Laminar MXene Membranes, *Process*, 2019, **7**, 751, DOI: 10.3390/PR7100751.

48 M. Krämer, Z. Besenyi, S. A. Burke, J. M. LeDue, Y. Miyahara, C. J. Shearer, A. D. Slattery, A. J. Stapleton, J. G. Shapter and C. T. Gibson, Accurate thickness measurement of graphene, *Nanotechnology*, 2016, **27**, 125704, DOI: 10.1088/0957-4484/27/12/125704.

49 P. Nemes-Incze, Z. Osváth, K. Kamarás and L. P. Biró, Anomalies in thickness measurements of graphene and

few layer graphite crystals by tapping mode atomic force microscopy, *Carbon*, 2008, **46**, 1435–1442, DOI: 10.1016/J.CARBON.2008.06.022.

50 A. Lipatov, H. Lu, M. Alhabeb, B. Anasori, A. Gruverman, Y. Gogotsi and A. Sinitskii, Elastic properties of 2D $Ti_3C_2T_x$ MXene monolayers and bilayers, *Sci. Adv.*, 2018, **4**(6), eaat0491.

51 X. Wang, X. Shen, Y. Gao, Z. Wang, R. Yu and L. Chen, Atomic-scale recognition of surface structure and intercalation mechanism of Ti_3C_2X, *J. Am. Chem. Soc.*, 2015, **137**(7), 2715–2721.

52 J. Halim, M. R. Lukatskaya, K. M. Cook, J. Lu, C. R. Smith, L. Å. Näslund, S. J. May, L. Hultman, Y. Gogotsi, P. Eklund and M. W. Barsoum, Transparent conductive two-dimensional titanium carbide epitaxial thin films, *Chem. Mater.*, 2014, **26**(7), 2374–2381.

53 J. Halim, K. M. Cook, P. Eklund, J. Rosen and M. W. Barsoum, XPS of cold pressed multilayered and freestanding delaminated 2D thin films of Mo_2TiC_2Tz and $Mo_2Ti_2C_3Tz$ (MXenes), *Appl. Surf. Sci.*, 2019, **494**, 1138–1147, DOI: 10.1016/J.APSUSC.2019.07.049.

54 O. Mashtalir, M. Naguib, V. N. Mochalin, Y. Dall'Agnese, M. Heon, M. W. Barsoum and Y. Gogotsi, Intercalation and delamination of layered carbides and carbonitrides, *Nat. Commun.*, 2013, 1–7, DOI: 10.1038/ncomms2664.

55 J. Halim, I. Persson, P. Eklund, P. O. Persson and J. Rosen, Sodium hydroxide and vacuum annealing modifications of the surface terminations of a Ti_3C_2 (MXene) epitaxial thin film, *RSC Adv.*, 2018, **8**(64), 36785–36790.

56 E. T. Hester, A. Y. C. Lin and C. W. Tsai, Effect of Floodplain Restoration on Photolytic Removal of Pharmaceuticals, *Environ. Sci. Technol.*, 2020, **54**, 3278–3287, DOI: 10.1021/ACS.EST.9B06850.

57 D. W. Kolpin, E. T. Furlong, M. T. Meyer, E. M. Thurman, S. D. Zaugg, L. B. Barber and H. T. Buxton, Pharmaceuticals, hormones, and other organic wastewater contaminants in U.S. streams, 1999–2000: A national reconnaissance, *Environ. Sci. Technol.*, 2002, **36**, 1202–1211, DOI: 10.1021/ES011055J.

58 Y. Li, J. B. Sallach, W. Zhang, S. A. Boyd and H. Li, Insight into the distribution of pharmaceuticals in soil-water-plant systems, *Water Res.*, 2019, **152**, 38–46, DOI: 10.1016/J.WATRES.2018.12.039.

59 L. M. Bexfield, P. L. Toccalino, K. Belitz, W. T. Foreman and E. T. Furlong, Hormones and Pharmaceuticals in Groundwater Used As a Source of Drinking Water Across the United States, *Environ. Sci. Technol.*, 2019, **53**, 2950–2960, DOI: 10.1021/ACS.EST.8B05592.

60 K. Manoli, L. M. Morrison, M. W. Sumarah, G. Nakhla, A. K. Ray and V. K. Sharma, Pharmaceuticals and pesticides in secondary effluent wastewater: Identification and enhanced removal by acid-activated ferrate(VI), *Water Res.*, 2019, **148**, 272–280, DOI: 10.1016/J.WATRES.2018.10.056.

61 S. Kim, F. Gholamirad, M. Yu, C. M. Park, A. Jang, M. Jang, N. Taheri-Qazvini and Y. Yoon, Enhanced adsorption performance for selected pharmaceutical compounds by sonicated $Ti_3C_2T_x$ MXene, *Chem. Eng. J.*, 2021, **406**, 126789, DOI: 10.1016/J.CEJ.2020.126789.

62 A. Miri-Jahromi, M. Didandeh and S. Shekarsokhan, Capability of MXene 2D material as an amoxicillin, ampicillin, and cloxacillin adsorbent in wastewater, *J. Mol. Liq.*, 2022, **351**, 118545, DOI: 10.1016/J.MOLLIQ.2022.118545.

63 A. A. Ghani, A. Shahzad, M. Moztahida, K. Tahir, H. Jeon, B. Kim and D. S. Lee, Adsorption and electrochemical regeneration of intercalated $Ti_3C_2T_x$ MXene for the removal of ciprofloxacin from wastewater, *Chem. Eng. J.*, 2021, **421**, 127780, DOI: 10.1016/J.CEJ.2020.127780.

64 S. Sukidpaneenid, C. Chawengkijwanich, C. Pokhum, T. Isobe, P. Opaprakasit and P. Sreearunothai, Multi-function adsorbent-photocatalyst MXene-TiO2 composites for removal of enrofloxacin antibiotic from water, *J. Environ. Sci.*, 2023, **124**, 414–428, DOI: 10.1016/J.JES.2021.09.042.

65 M. Xu, C. Huang, J. Lu, Z. Wu, X. Zhu, H. Li, L. Xiao and Z. Luo, Optimizing Adsorption of 17α-Ethinylestradiol from Water by Magnetic MXene Using Response Surface Methodology and Adsorption Kinetics, Isotherm, and Thermodynamics Studies, *Molecules*, 2021, **26**(11), 3150.

66 M. Bounaas, A. Bouguettoucha, D. Chebli, J. M. Gatica and H. Vidal, Role of the wild carob as biosorbent and as precursor of a new high-surface-area activated carbon for the adsorption of methylene blue, *Arabian J. Sci. Eng.*, 2020, **46**, 325–341, DOI: 10.1007/s13369-020-04739-5.

67 Y. Hao, R. Gao, L. Shi, D. Liu, Y. Tang and Z. Guo, Water-compatible magnetic imprinted nanoparticles served as solid-phase extraction sorbents for selective determination of trace 17β-estradiol in environmental water samples by liquid chromatography, *J. Chromatogr. A*, 2015, **1396**, 7–16, DOI: 10.1016/j.chroma.2015.03.083.

68 X. Dao, H. Hao, J. Bi, S. Sun and X. Huang, Surface Complexation Enhanced Adsorption of Tetracycline by alk-MXene, *Ind. Eng. Chem. Res.*, 2022, **61**, 6028–6036, DOI: 10.1021/acs.iecr.2c00037.

69 B. C. Almroth, J. Cartine, C. Jönander, M. Karlsson, J. Langlois, M. Lindström, J. Lundin, N. Melander, A. Pesqueda, I. Rahmqvist and J. Renaux, Assessing the effects of textile leachates in fish using multiple testing methods: from gene expression to behavior, *Ecotoxicol. Environ. Saf.*, 2021, **207**, 111523.

70 G. Zou, J. Guo, Q. Peng, A. Zhou, Q. Zhang and B. Liu, Synthesis of urchin-like rutile titania carbon nanocomposites by iron-facilitated phase transformation of MXene for environmental remediation, *J. Mater. Chem. A*, 2015, **4**, 489–499, DOI: 10.1039/C5TA07343J.

71 B. Sun, X. Dong, H. Li, Y. Shang, Y. Zhang, F. Hu, S. Gu, Y. Wu, T. Gao and G. Zhou, Surface charge engineering for two-dimensional Ti_2CT_x MXene for highly efficient and selective removal of cationic dye from aqueous solution, *Sep. Purif. Technol.*, 2021, **272**, 118964, DOI: 10.1016/J.SEPPUR.2021.118964.

72 B. M. Jun, J. Heo, N. Taheri-Qazvini, C. M. Park and Y. Yoon, Adsorption of selected dyes on $Ti_3C_2T_x$ MXene and Al-based

metal-organic framework, *Ceram. Int.*, 2020, **46**(3), 2960–2968.

73 D. Ghosh and K. G. Bhattacharyya, Adsorption of methylene blue on kaolinite, *Appl. Clay Sci.*, 2002, **20**, 295–300, DOI: 10.1016/S0169-1317(01)00081-3.

74 Z. Wei, Z. Peigen, T. Wubian, Q. Xia, Z. Yamei and S. ZhengMing, Alkali treated $Ti_3C_2T_x$ MXenes and their dye adsorption performance, *Mater. Chem. Phys.*, 2018, **206**, 270–276, DOI: 10.1016/J.MATCHEMPHYS.2017.12.034.

75 C. Peng, P. Wei, X. Chen, Y. Zhang, F. Zhu, Y. Cao, H. Wang, H. Yu and F. Peng, A hydrothermal etching route to synthesis of 2D MXene (Ti3C2, Nb2C): Enhanced exfoliation and improved adsorption performance, *Ceram. Int.*, 2018, **44**, 18886–18893, DOI: 10.1016/J.CERAMINT.2018.07.124.

76 K. Li, G. Zou, T. Jiao, R. Xing, L. Zhang, J. Zhou, Q. Zhang and Q. Peng, Self-assembled MXene-based nanocomposites *via* layer-by-layer strategy for elevated adsorption capacities, *Colloids Surf., A*, 2018, **553**, 105–113, DOI: 10.1016/J.COLSURFA.2018.05.044.

77 M. Vakili, G. Cagnetta, J. Huang, G. Yu and J. Yuan, Synthesis and Regeneration of A MXene-Based Pollutant Adsorbent by Mechanochemical Methods, *Molecules*, 2019, **24**, 2478, DOI: 10.3390/MOLECULES24132478.

78 Y. Lei, Y. Cui, Q. Huang, J. Dou, D. Gan, F. Deng, M. Liu, X. Li, X. Zhang and Y. Wei, Facile preparation of sulfonic groups functionalized Mxenes for efficient removal of methylene blue, *Ceram. Int.*, 2019, **45**, 17653–17661, DOI: 10.1016/J.CERAMINT.2019.05.331.

79 Z. Zhu, M. Xiang, L. Shan, T. He and P. Zhang, Effect of temperature on methylene blue removal with novel 2D-Magnetism titanium carbide, *J. Solid State Chem.*, 2019, **280**, 120989, DOI: 10.1016/J.JSSC.2019.120989.

80 C. Cai, R. Wang, S. Liu, X. Yan, L. Zhang, M. Wang, Q. Tong and T. Jiao, Synthesis of self-assembled phytic acid-MXene nanocomposites *via* a facile hydrothermal approach with elevated dye adsorption capacities, *Colloids Surf., A*, 2020, **589**, 124468, DOI: 10.1016/J.COLSURFA.2020.124468.

81 M. Kadhom, K. Kalash and M. Al-Furaiji, Performance of 2D MXene as an adsorbent for malachite green removal, *Chemosphere*, 2022, **290**, 133256, DOI: 10.1016/J.CHEMOSPHERE.2021.133256.

82 J. Xu, G. Zeng, Q. Lin, Y. Gu, X. Wang, Z. Feng and A. Sengupta, Application of 3D magnetic nanocomposites: MXene-supported Fe_3O_4@CS nanospheres for highly efficient adsorption and separation of dyes, *Sci. Total Environ.*, 2022, **822**, 153544, DOI: 10.1016/J.SCITOTENV.2022.153544.

83 L. Zhang, D. Huang, P. Zhao, G. Yue, L. Yang and W. Dan, Highly efficient methylene blue removal by TMAOH delaminated $Ti_3C_2T_x$ MXene suspension and the mechanistic aspect, *Sep. Purif. Technol.*, 2022, **288**, 120718, DOI: 10.1016/J.SEPPUR.2022.120718.

84 J. Stejskal, Interaction of conducting polymers, polyaniline and polypyrrole, with organic dyes: polymer morphology control, dye adsorption and photocatalytic decomposition, *Chem. Zvesti*, 2020, **74**(1), 1–54, DOI: 10.1007/s11696-019-00982-9.

85 F. F. Ma, D. Zhang, N. Zhang, T. Huang and Y. Wang, Polydopamine-assisted deposition of polypyrrole on electrospun poly(vinylidene fluoride) nanofibers for bidirectional removal of cation and anion dyes, *Chem. Eng. J.*, 2018, **354**, 432–444, DOI: 10.1016/j.cej.2018.08.048.

86 X. Y. Shi, M. H. Gao, W. W. Hu, D. Luo, S. Z. Hu, T. Huang, N. Zhang and Y. Wang, Largely enhanced adsorption performance and stability of MXene through *in situ* depositing polypyrrole nanoparticles, *Sep. Purif. Technol.*, 2022, **287**, 120596, DOI: 10.1016/J.SEPPUR.2022.120596.

87 C. Hao, G. Li, G. Wang, W. Chen and S. Wang, Preparation of acrylic acid modified alkalized MXene adsorbent and study on its dye adsorption performance, *Colloids Surf., A*, 2022, **632**, 127730, DOI: 10.1016/J.COLSURFA.2021.127730.

88 Y. Yan, H. Han, Y. Dai, H. Zhu, W. Liu, X. Tang, W. Gan and H. Li, Nb2CTxMXene Nanosheets for Dye Adsorption, *ACS Appl. Nano Mater.*, 2021, **4**, 11763–11769, DOI: 10.1021/ACSANM.1C02339.

89 Z. Wu, W. Deng, S. Tang, E. Ruiz-Hitzky, J. Luo and X. Wang, Pod-inspired MXene/porous carbon microspheres with ultrahigh adsorption capacity towards crystal violet, *Chem. Eng. J.*, 2021, **426**, 130776, DOI: 10.1016/J.CEJ.2021.130776.

90 M. Rethinasabapathy, G. Bhaskaran, B. Park, J. Y. Shin, W. S. Kim, J. Ryu and Y. S. Huh, Iron oxide (Fe_3O_4)-laden titanium carbide ($Ti_3C_2T_x$) MXene stacks for the efficient sequestration of cationic dyes from aqueous solution, *Chemosphere*, 2022, **286**, 131679, DOI: 10.1016/J.CHEMOSPHERE.2021.131679.

91 R. Long, Z. Yu, Q. Tan, X. Feng, X. Zhu, X. Li and P. Wang, Ti3C2 MXene/NH2-MIL-88B(Fe): Research on the adsorption kinetics and photocatalytic performance of an efficient integrated photocatalytic adsorbent, *Appl. Surf. Sci.*, 2021, **570**, 151244, DOI: 10.1016/J.APSUSC.2021.151244.

92 J. Qu, D. Teng, X. Zhang, Q. Yang, P. Li and Y. Cao, Preparation and regulation of two-dimensional $Ti_3C_2T_x$ MXene for enhanced adsorption–photocatalytic degradation of organic dyes in wastewater, *Ceram. Int.*, 2022, **48**, 14451–14459, DOI: 10.1016/J.CERAMINT.2022.01.338.

93 H. K. Gill and H. Garg, Pesticide: environmental impacts and management strategies, *Pestic.: Toxic Aspects*, 2014, **8**, 187.

94 S. Mostafalou and M. Abdollahi, Concerns of environmental persistence of pesticides and human chronic diseases, *Clin. Exp. Pharmacol.*, 2012, S5-e002, DOI: 10.4172/2161-1459.S5-e002.

95 T. Guo, Y. Lei, X. Hu, G. Yang, J. Liang, Q. Huang, X. Li, M. Liu, X. Zhang and Y. Wei, Hydrothermal synthesis of MXene-MoS2 composites for highly efficient removal of pesticides, *Appl. Surf. Sci.*, 2022, **588**, 152597.

96 Endocrine Disruptors, National Institute of Environmental Health Sciences, cited 7 Feb 2021, available from: https://

www.niehs.nih.gov/health/topics/agents/endocrine/index.cfm.

97 Research NC for T. Endocrine Disruptor Knowledge Base, FDA, 2019, cited 7 Feb 2021, available from: https://www.fda.gov/science-research/bioinformatics-tools/endocrine-disruptor-knowledge-base.

98 M. N. H. Rozaini, W. Kiatkittipong, B. Saad, N. Yahaya, M. S. Shaharun, S. S. Sangu, M. S. Mohamed Saheed, Y. F. Wong, M. Mohamad, N. S. Sambudi and J. W. Lim, Green adsorption–desorption of mixed triclosan, triclocarban, 2-phenylphenol, bisphenol A and 4-tert-octylphenol using MXene encapsulated polypropylene membrane protected micro-solid-phase extraction device in amplifying the HPLC analysis, *Microchem. J.*, 2021, **170**, 106695, DOI: 10.1016/J.MICROC.2021.106695.

99 Q. Wang, Y. Xiong, J. Xu, F. Dong and Y. Xiong, Oxidation-Resistant Cyclodextrin-Encapsulated-MXene/Poly (*N*-isopropylacrylamide) composite hydrogel as a thermosensitive adsorbent for phenols, *Sep. Purif. Technol.*, 2022, **286**, 120506, DOI: 10.1016/J.SEPPUR.2022.120506.

100 F. Meng, M. Seredych, C. Chen, V. Gura, S. Mikhalovsky, S. Sandeman, G. Ingavle, T. Ozulumba, L. Miao, B. Anasori and Y. Gogotsi, MXene Sorbents for Removal of Urea from Dialysate: A Step toward the Wearable Artificial Kidney, *ACS Nano*, 2018, **12**(10), 10518–10528.

101 L. Wu, X. Lu, Dhanjai, Z. S. Wu, Y. Dong, X. Wang, S. Zheng and J. Chen, 2D transition metal carbide MXene as a robust biosensing platform for enzyme immobilization and ultrasensitive detection of phenol, *Biosens. Bioelectron.*, 2018, **107**, 69–75, DOI: 10.1016/J.BIOS.2018.02.021.

102 Y. Ying, Y. Liu, X. Wang, Y. Mao, W. Cao, P. Hu and X. Peng, *ACS Appl. Mater. Interfaces*, 2015, **7**, 1795.

103 Y. Tang, C. Yang and W. Que, A novel two-dimensional accordion-like titanium carbide (MXene) for adsorption of Cr(VI) from aqueous solution, *J. Adv. Dielectr.*, 2018, **8**, 1850035.

104 P. Karthikeyan, K. Ramkumar, K. Pandi, A. Fayyaz, S. Meenakshi and C. M. Park, Effective removal of Cr(VI) and methyl orange from the aqueous environment using two-dimensional (2D) $Ti_3C_2T_x$ MXene nanosheets, *Ceram. Int.*, 1 February 2021, **47**(3), 3692–3698.

105 A. Kong, Yawei Sun, Mao Peng, Hongzhi Gu Yan Fu Jinli Zhang Wei Li, Amino-functionalized MXenes for efficient removal of Cr(VI), *Colloids Surf., A*, 2021, **617**, 126388.

106 K. Fu, X. Liu, D. Yu, J. Luo, Z. Wang and J. C. Crittenden, Highly efficient and selective Hg(II) removal from water using multilayered Ti3C2Ox MXene *via* adsorption coupled with catalytic reduction mechanism, *Environ. Sci. Technol.*, 2020, **54**, 16212–16220.

107 A. Shahzad, K. Rasool, W. Miran, M. Nawaz, J. Jang, K. A. Mahmoud and D. S. Lee, Mercuric ion capturing by recoverable titan titanium carbide magnetic nanocomposite, *J. Hazard. Mater.*, 2018, **344**, 811–818.

108 A. Shahzad, J. Jang, S. R. Lim and D. S. Lee, Unique selectivity and rapid uptake of molybdenum-disulfide-functionalized MXene nanocomposite for mercury adsorption, *Environ. Res.*, 2020, **182**, 109005.

109 A. Shahzad, K. Rasool, J. Iqbal, J. Jang, Y. Lim, B. Kim, J. M. Oh and D. S. Lee, MXsorption of mercury: Exceptional reductive behavior of titanium carbide/carbonitride MXenes, *Environ. Res.*, 2022, **2051**, 112532.

110 Q. Peng, J. Guo, Q. Zhang, J. Xiang, B. Liu, A. Zhou, R. Liu and Y. Tian, Unique lead adsorption behavior of activated hydroxyl group in two-dimensional titanium carbide, *J. Am. Chem. Soc.*, 2014, **136**, 4113–4116.

111 Y. Dong, D. Sang, C. He, X. Sheng and L. Lei, Mxene/alginate composites for lead and copper ion removal from aqueous solutions, *RSC Adv.*, 2019, **9**, 29015–29022.

112 G. Zhang, T. Wang, Z. Xu, M. Liu, C. Shen and Q. Meng, Synthesis of amino-functionalized $Ti_3C_2T_x$ MXene by alkalization-grafting modification for efficient lead adsorption, *Chem. Commun.*, 2020, **56**, 11283–11286.

113 A. K. Fard, G. McKay, R. Chamoun, T. Rhadfi, H. Preud'Homme and M. A. Atieh, *Chem. Eng. J.*, 2017, **317**, 331–342.

114 K. N. Zhang, C. Z. Wang, Q. F. Lü and M. H. Chen, Enzymatic hydrolysis lignin functionalized $Ti_3C_2T_x$ nanosheets for effective removal of MB and Cu^{2+} ions, *Int. J. Biol. Macromol.*, 2022, **209**(Pt A), 680–691.

115 B. M. Jun, S. Kim, H. Rho, C. M. Park and Y. Yoon, Ultrasound-assisted $Ti_3C_2T_x$ MXene adsorption of dyes: Removal performance and mechanism analyses *via* dynamic light scattering, *Chemosphere*, 2020, **254**, 126827, DOI: 10.1016/J.CHEMOSPHERE.2020.126827.

116 B. M. Jun, J. Han, C. M. Park and Y. Yoon, Ultrasonic degradation of selected dyes using $Ti_3C_2T_x$ MXene as a sonocatalyst, *Ultrason. Sonochem.*, 2020, **64**, 104993, DOI: 10.1016/J.ULTSONCH.2020.104993.

117 H. Lei, Z. Hao, K. Chen, K. Chen, Y. Chen, J. Zhang, Z. Hu, Y. Song, P. Rao, Q. Huang and Q. Huang, Insight into Adsorption Performance and Mechanism on Efficient Removal of Methylene Blue by Accordion-like V_2CT_xMXene, *J. Phys. Chem. Lett.*, 2020, **11**, 4253–4260.

118 P. Zhang, M. Xiang, H. Liu, C. Yang and S. Deng, Novel Two-Dimensional Magnetic Titanium Carbide for Methylene Blue Removal over a Wide pH range: Insight into Removal Performance and Mechanism, *ACS Appl. Mater. Interfaces*, 2019, **11**, 24027–24036, DOI: 10.1021/ACSAMI.9B04222.

119 C. Duan, T. Ma, J. Wang and Y. Zhou, Removal of heavy metals from aqueous solution using carbon-based adsorbents: A review, *J. Water Process. Eng.*, 2020, **37**, 101339, DOI: 10.1016/J.JWPE.2020.101339.

120 A. Shahzad, K. Rasool, W. Miran, M. Nawaz, J. Jang, K. A. Mahmoud and D. S. Lee, Two-Dimensional $Ti_3C_2T_x$ MXene Nanosheets for Efficient Copper Removal from Water, *ACS Sustainable Chem. Eng.*, 2017, **5**, 11481–11488, DOI: 10.1021/ACSSUSCHEMENG.7B02695.

121 Y. Ying, Y. Liu, X. Wang, Y. Mao, W. Cao, P. Hu and X. Peng, Two-dimensional titanium carbide for efficiently reductive removal of highly toxic chromium(VI) from water, *ACS Appl.*

Mater. Interfaces, 2015, **7**, 1795–1803, DOI: **10.1021/AM5074722**.

122 L. Wang, H. Song, L. Yuan, Z. Li, Y. Zhang, J. K. Gibson, L. Zheng, Z. Chai and W. Shi, Efficient U(VI) Reduction and Sequestration by Ti2CTx MXene, *Environ. Sci. Technol.*, 2018, **52**, 10748–10756, DOI: **10.1021/ACS.EST.8B03711**.

123 A. Shahzad, J. Jang, S. R. Lim and D. S. Lee, Unique selectivity and rapid uptake of molybdenum-disulfide-functionalized MXene nanocomposite for mercury adsorption, *Environ. Res.*, 2020, **182**, 109005, DOI: **10.1016/J.ENVRES.2019.109005**.

124 X. Feng, Z. Yu, R. Long, X. Li, L. Shao, H. Zeng, G. Zeng and Y. Zuo, Self-assembling 2D/2D (MXene/LDH) materials achieve ultra-high adsorption of heavy metals Ni^{2+} through terminal group modification, *Sep. Purif. Technol.*, 2020, **253**, 117525, DOI: **10.1016/J.SEPPUR.2020.117525**.

125 A. Jastrzębska, A. Szuplewska, T. Wojciechowski, M. Chudy, W. Ziemkowska, L. Chlubny, A. Rozmysłowska and A. Olszyna, In vitro studies on cytotoxicity of delaminated Ti3C2 MXene, *J. Hazard. Mater.*, 2017, **339**, 1–8.

126 H. Lin, S. Gao, C. Dai, Y. Chen and J. Shi, A two-dimensional biodegradable niobium carbide (MXene) for photothermal tumor eradication in NIR-I and NIR-II biowindows, *J. Am. Chem. Soc.*, 2017, **139**, 16235–16247.

127 C. J. Zhang, S. Pinilla, N. McEvoy, C. P. Cullen, B. Anasori, E. Long, S.-H. Park, A. Seral-Ascaso, A. Shmeliov, D. Krishnan, C. Morant, X. Liu, G. S. Duesberg, Y. Gogotsi and V. Nicolosi, Oxidation Stability of Colloidal Two-Dimensional Titanium Carbides (MXenes), *Chem. Mater.*, 2017, **29**, 4848–4856.

128 X. Gao, H. Liu, D. Wang and J. Zhang, Graphdiyne: synthesis, properties, and applications, *Chem. Soc. Rev.*, 2019, **48**, 908–936, DOI: **10.1039/C8CS00773J**.

129 K. A. Mohamed Eid and M. A. Aboubakr, *Carbon Nitride Nanostructures for Sustainable Energy Production and*, Royal Society of Chemistry, 1st edn, 2021.

130 Q. Lu, K. Eid, W. Li, A. M. Abdullah, G. Xu and R. S. Varma, Engineering graphitic carbon nitride ($g\text{-}C_3N_4$) for catalytic reduction of CO_2 to fuels and chemicals: strategy and mechanism, *Green Chem.*, 2021, **23**, 5394–5428, DOI: **10.1039/D1GC01303C**.

131 Q. Lu, W. Li, L. Gai and K. Eid, CHAPTER 3:Template-based Fabrication of Porous Carbon Nitride Nanostructures for Electrochemical Energy Conversion, *RSC Nanosci. Nanotechnol.*, 2021, 80–126, DOI: **10.1039/9781839164606-00080**.

132 M. Gu, Z. Dai, X. Yan, J. Ma, Y. Niu, W. Lan, X. Wang and Q. Xu, Comparison of toxicity of Ti_3C_2 and Nb_2C Mxene quantum dots (QDs) to human umbilical vein endothelial cells, *J. Appl. Toxicol.*, 2021, **41**, 745–754, DOI: **10.1002/JAT.4085**.